Biochimica et Biophysica Acta 1808 (2011) 955–970

Contents lists available at ScienceDirect

Biochimica et Biophysica Acta

journal homepage: www.elsevier.com/locate/bbamem

Review

Structural insight into the mitochondrial protein import system[☆]

Toshiya Endo*, Koji Yamano, Shin Kawano

Department of Chemistry, Graduate School of Science, Nagoya University, Chikusa-ku, Nagoya 464-8602, Japan

A R T I C L E   I N F O

Article history:
Received 15 May 2010
Received in revised form 13 July 2010
Accepted 19 July 2010
Available online 23 July 2010

Keywords:
Protein import
Mitochondria
Translocator
Receptor
X-ray structure
NMR structure

A B S T R A C T

Mitochondrial functions rely on precise and efficient transport of 1000–1500 different mitochondrial proteins from the cytosol to appropriate mitochondrial subcompartments. Those mitochondrial protein transport processes are mediated by the dedicated mitochondrial protein import system comprised of translocators in the outer and inner mitochondrial membranes and soluble factors in the cytosol, intermembrane space, and matrix. In the last decade, high-resolution structures of many of the components of the mitochondrial protein import machineries have become available, which has significantly advanced our understanding of the molecular mechanisms of mitochondrial protein transport. Here we review the currently available high-resolution structures of the components of the mitochondrial protein import machineries that afford structural and mechanistic insight into how the mitochondrial import system works. This article is part of a Special Issue entitled Protein translocation across or insertion into membranes.

Contents

[☆] This article is part of a Special Issue entitled Protein translocation across or insertion into membranes.

* Corresponding author. Tel.: +81 52 789 2490; fax: +81 52 789 2947.
E-mail address: endo@biochem.chem.nagoya-u.ac.jp (T. Endo).

0005-2736/$ – see front matter © 2010 Elsevier B.V. All rights reserved.
doi:10.1016/j.bbamem.2010.07.018

1. Introduction

Mitochondria are essential organelles in eukaryotic cells that consist of four subcompartments, the outer and inner membranes, the intermembrane space (IMS), and innermost matrix. Mitochondria contain about 1000–1500 different proteins, most of which are synthesized as precursor proteins in the cytosol and imported into mitochondria. Import and subsequent intramitochondrial sorting of mitochondrial proteins are mediated by membrane-protein complexes called translocators in the outer and inner membranes and soluble factors in the cytosol, IMS, and matrix [1–4]. Most mitochondrial proteins enter mitochondria via the outer-membrane translocator, the TOM40 complex. Then the protein-sorting pathway branches out for different mitochondrial subcompartments with the aid of distinct sorting-specific import machineries (Fig. 1). The TIM23 complex in the inner membrane mediates sorting of precursor proteins with an N-terminal cleavable presequence to the matrix and inner membrane. The TIM22 complex in the inner membrane facilitates insertion of polytopic membrane proteins without a presequence into the inner membrane. The TOB/SAM complex in the outer membrane mediates assembly of β-barrel membrane proteins into the outer membrane [5–7]. Tim40/Mia40 and Erv1 constitute a disulfide relay system in the IMS to facilitate import and oxidative folding of mainly small soluble proteins in the IMS [8–11].

Mitochondrial precursor proteins are classified into two groups on the basis of their mitochondrial-targeting signals, which are recognized by distinct receptors of the translocators. Most matrix proteins and some inner membrane proteins are synthesized as precursor proteins with an N-terminal presequence, which contains a mitochondrial-targeting signal and is cleaved off by the processing peptidase in the matrix upon import [12,13]. On the other hand, polytopic inner membrane proteins, soluble IMS proteins, and outer-membrane proteins are mainly synthesized without a cleavable presequence, but contain internal targeting signals within their mature parts.

In the last decade, information on the structural aspects of mitochondrial import systems has been accumulated. In particular, high-resolution structures have become available for many components of the mitochondrial protein import system, which contributed to enhancement of our understanding of the mechanisms of protein import and sorting on the basis of the structures. In this review, we will give a brief survey of the currently available high-resolution structures of the components of the protein import machineries and correlate the structural information with their functions in the mitochondrial protein trafficking.

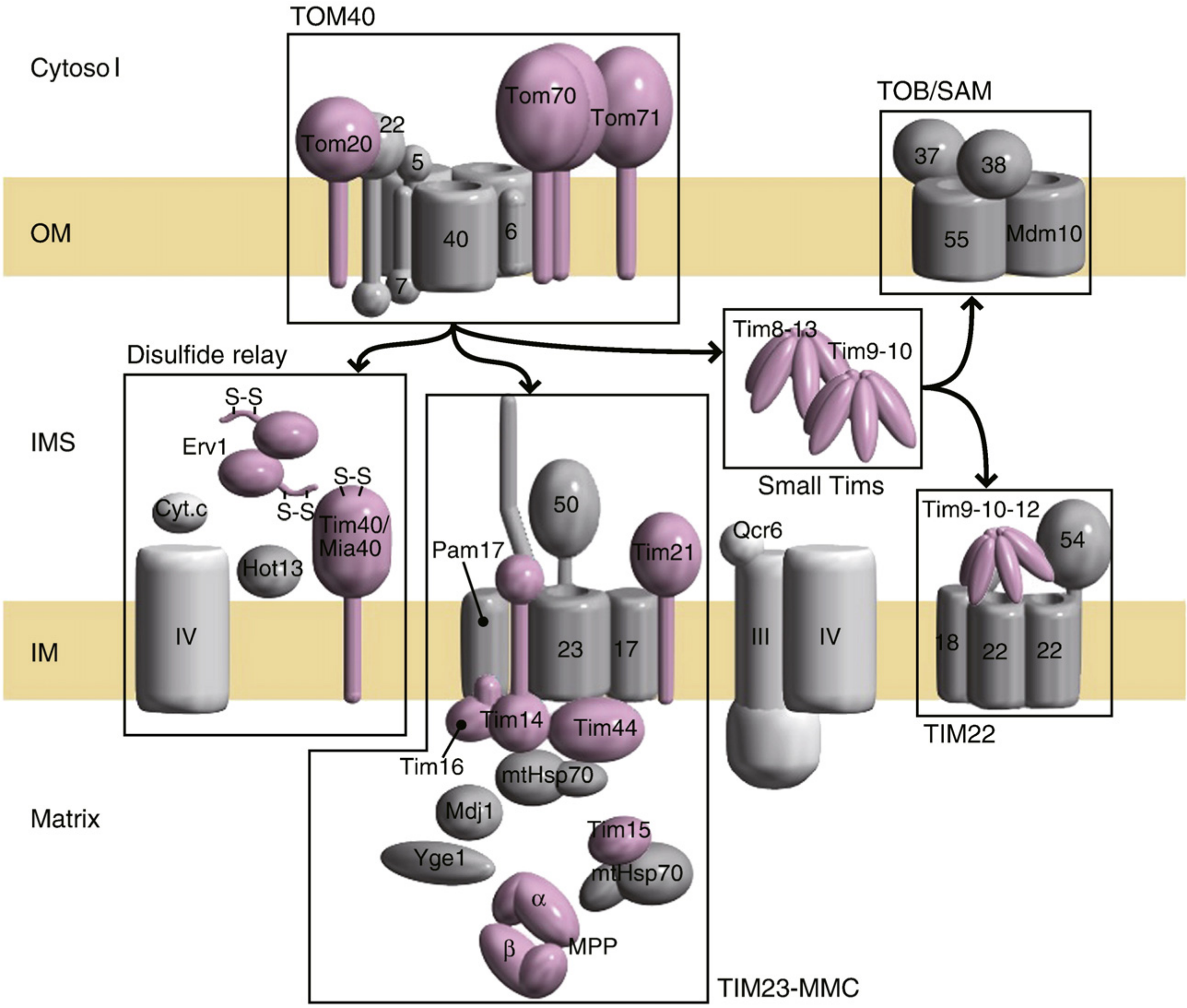

Fig. 1. Mitochondrial protein import pathways and translocators. The components whose high-resolution structures are available are shown in pink. TOM40, the TOM40 complex (40, Tom40; 22, Tom22; 7, Tom7; 6, Tom6; 5, Tom5); TOB/SAM, the TOB/SAM complex (55, Tob55/Sam50; 38, Tom38/Tob38/Sam35; 37, Mas37/Sam37/Tom37); Disulfide relay, the disulfide relay system (Cyt. c, cytochrome *c*; IV, the respiratory chain complex IV); TIM23–MMC, the TIM23 complex and MMC proteins (50, Tim50; 23, Tim23; 17, Tim17); TIM22, the TIM22 complex (54, Tim54; 22, Tim22; 18, Tim18); III, the respiratory chain complex III.

2. The TOM40 complex

2.1. The TOM40 complex

The TOM40 complex in the outer membrane functions as a major entry gate for most mitochondrial proteins by facilitating their translocation across the outer membrane (Fig. 1). The TOM40 complex consists of the core complex comprised of Tom40, Tom22, Tom5, Tom6, and Tom7, and peripherally associated receptors, Tom20 and Tom70 (and a minor component Tom71) (Fig. 1). Single particle electron microscopy (EM) analyses revealed that the intact *Neurospora crassa* TOM40 complex solubilized with dedecylmaltoside has two to three pores as protein-conducting channels [14]. When receptor subunits Tom20 and Tom70 were removed, the core TOM40 complexes from *N. crassa* and yeast showed predominantly double ring structures containing two pores with a diameter of ~21 Å (*N. crassa*) or 20–30 Å (yeast) and a height of ~70 Å (*N. crassa*) [15,16]. Recent cryo-EM analyses further revealed that the TOM40 complex containing Tom20, not Tom70, shows a triangular structure, measuring 145 Å on edge, with three elliptical pores (~25 × 15 Å) and probably three Tom22 and around two Tom20 molecules in the peripheral and central protrusions, respectively [17]. The TOM40 channel likely consists of the β-barrel pore of Tom40, which is stabilized by the other subunits including Tom22 [18,19]. The estimated diameter of the TOM40 pore is large enough to accept two polypeptide segments in a loop conformation in its interior [15–19].

2.2. Tom20

The TOM40 complex in animals and fungi contains receptor subunits, Tom20 and Tom70 (and Tom71), which recognize mitochondrial-targeting signals. Tom20 contains a single transmembrane (TM) segment near the N-terminus to be anchored to the outer membrane, exposing the C-terminal receptor domain to the cytosol [20–22]. Plant mitochondria contain functional counterparts for Tom20, which take the reverse orientation or N_{out}–C_{in} topology to be integrated in the outer membrane [23].

Tom20 is the major import receptor that preferentially recognizes the targeting signals of presequence-containing proteins. Typical mitochondrial presequences are variable in length and lack any consensus sequences [12]. Yet, they are rich in both hydrophobic and hydrophilic, often basic residues that can form amphiphilic helices, with the charged residues on one side and the hydrophobic residues on the other [24–26]. Rat Tom20 was the first membrane-bound protein import receptor whose high-resolution structure was determined [27]. The receptor core domain (residues 51–145) of rat Tom20 in a complex with an 11-residue peptide (residues 12–22) derived from the rat aldehyde dehydrogenase (ALDH) presequence (residues 1–22) was analyzed by NMR to determine its high-resolution structure. The structure of the Tom20 core domain consists of five α-helices, three of which form a hydrophobic concave groove that accommodates the presequence peptide. The bound ALDH presequence peptide takes an amphiphilic helical structure with its hydrophobic side in contact with the hydrophobic groove of Tom20. Since the binding groove of Tom20 is shallow, the hydrophilic residues of the presequence peptide on the other side of the helix are exposed to the aqueous solvent, which should be energetically favorable. This is in contrast to the receptor domain of the bacterial signal recognition particle (Ffh), which has a deep hydrophobic groove to recognize fully hydrophobic helical structures of bacterial secretory signal peptides. Although taking a reversed orientation, the NMR structure of the receptor domain of *Arabidopsis thaliana* Tom20 counterpart also has a hydrophobic groove that is conserved among plant Tom20 counterparts [23]. The NMR signals of the residues constituting the hydrophobic groove were affected by addition of the presequence peptides, indicating that mitochondrial presequences indeed bind to this groove [23].

The size of the hydrophobic groove of rat Tom20 suggests that an amphiphilic helix of the presequence peptide bound to Tom20 is at most two turns long, and therefore sequences recognized by Tom20 are as short as 8 amino-acid residues [27]. Indeed, when various presequence peptides were analyzed for their interactions with the Tom20 core domain by NMR, binding elements for Tom20 in the presequence peptides are 6–8 residues long [28]. Interestingly however, positions of the elements recognized by Tom20 are variable in the presequences, either near the N-terminus or at the C-terminus [28]. The Tom20-binding elements identified in different presequence peptides were found to exhibit a common pattern described as $\phi\chi\chi\phi\phi$ (ϕ is a hydrophobic amino acid, and χ is any amino acid). When any of the three Leu in this motif ($L_1S_2R_3L_4L_5$) of the ALDH presequence was replaced with hydrophilic Gln, binding affinity for rat Tom20 decreased [27]. The Leu to Ala mutations in the presequences were also found to decrease their affinity for Tom20, while retaining their ability to import passenger proteins to mitochondria both *in vitro* and *in vivo* [29]. This may underscore the importance of the residual Tom20-bypass import [30] in particular *in vivo* and/or even weak binding of mutated presequences to Tom20 may be sufficient to enter the mitochondrial import pathway under the conditions where receptor binding is not rate-limiting [31].

In the NMR structure of the complex of the rat Tom20 core domain and ALDH presequence peptide, the peptide appeared to have some residual mobility in the Tom20 groove, rendering the precise position and structure of the peptide elusive. To overcome this problem in precise structural determination, Saitoh et al. tethered the presequence peptide to Tom20 by an intermolecular disulfide bond, which allowed the peptide to bind to Tom20 tightly, for X-ray crystallography [32]. Two distinct crystal structures of the complex of Tom20 and the ALDH presequence peptide were obtained at resolutions of 1.9 Å and 2.1 Å, which suggest the presence of a dynamic equilibrium among two or more bound states of the presequence peptide in its complex with Tom20 (Fig. 2). Although the ALDH presequence has three Leu residues required for the interactions with Tom20, Tom20 is equipped with only two hydrophobic subsites in the concave hydrophobic groove. Indeed one of the three Leu residues of the ALDH presequence, L1 or L5 in the $L_1S_2R_3L_4L_5$ motif, has few contacts with Tom20 in the two distinct structures of the Tom20-presequence complex (Fig. 2). On the basis of those structures, the authors suggested that the presequence peptide could take e.g. two different relative geometries to the hydrophobic groove of Tom20, allowing the two key hydrophobic residues in the $\phi\chi\chi\phi\phi$ motif formed by diverse presequences to be best recognized by Tom20 without an induced fit mechanism [32].

Which subunits, if any, recognize the positively charged side of the amphiphilic helix of the presequence bound to Tom20? Possible candidates are the cytosolic domains of Tom22 [33] and Tom5 [34], both of which contain some acidic amino-acid residues. Tom22 spans the outer membrane by its central TM segment, with its N-terminal and C-terminal domains exposed to the cytosol and IMS, respectively. Recent analyses on the *in vitro* protein import of various precursor proteins into mitochondria lacking one of the two cytosolic domains of Tom20 and Tom22 revealed surprising similarity for substrate specificities between Tom20 and Tom22 [35]. This strongly suggests that those two receptor subunits are involved in the same pathway of targeting signal recognition in import, which is consistent with the model that Tom20 and Tom22 recognize the amphiphilic helix formed by the same presequence simultaneously, Tom20 recognizing the hydrophobic side and Tom22 the hydrophilic side [33]. The acidic domain of Tom5 may guide the positively charged presequence to the narrow Tom40 channel [34].

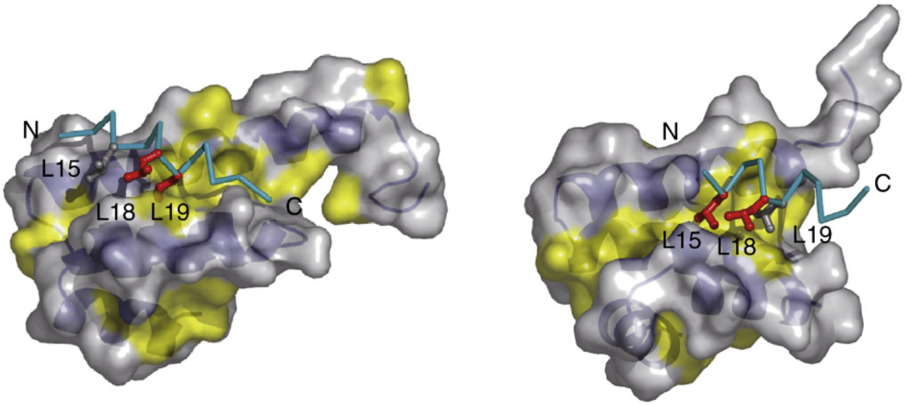

Fig. 2. Comparison of the two crystal structures of the Tom20-presequence complex (2VIT, 2VIS). Left panel, A-linker structure; right panel, Y-linker structure. A-linker and Y-linker possess Ala and Tyr at the first residue of the 4-residue linker segment following the ALDH presequence-derived peptide (GPRLSRLLS). Cys at the end of the linker segment forms a disulfide bond with Cys100 in Tom20. Semi-transparent molecular surface shows the structures of the rat Tom20 core domain with hydrophobic residues (Ile, Leu, Met, Tyr, Phe, Val, and Trp) in yellow. The main chains of the bound ALDH presequence peptides are shown in blue, and side chains of the three Leu residues of L1, L4 and L5 in the $L_1S_2R_3L_4L_5$ motif are shown in the rod model (the side chains in contact with Tom20 are indicated in magenta).

2.3. Tom70

Tom70 is anchored to the outer membrane by its N-terminal TM segment and exposes the large C-terminal receptor domain to the cytosol [36–38]. In contrast to Tom20, Tom70 preferentially recognizes presequence-less inner membrane proteins with multiple TM segments such as metabolic carrier proteins. Although several presequence-containing proteins also require Tom70 for their import into mitochondria *in vitro*, targeting information in the presequence of those precursor proteins is still decoded by Tom20, and Tom70 functions solely as a chaperone to prevent them from aggregate formation [39]. Tom70 also functions as a docking site for cytosolic chaperones such as Hsp70 (in yeast and mammals) and Hsp90 (mammals) that carry aggregate-prone mitochondrial precursor proteins across the cytosol [40].

The crystal structure of the cytosolic domain of yeast Tom70 (residues 39–617) was determined at resolution of 3.0 Å; it consists of 26 α-helices, the majorities of which constitute 11 tetratricopeptide repeat (TPR) motifs. The 11 TPR motifs are clustered into two sub-domains connected by a flexible linker, which is disordered in the crystal structure [41]. The C-terminal sub-domain contains a large putative substrate precursor-binding pocket, which consists of many conserved hydrophobic residues in the interior and some charged residues at the opening (Fig. 3). This hydrophobic pocket may mediate recognition of mitochondrial-targeting signals of presequence-less substrate precursor proteins and/or interactions with exposed hydrophobic regions of aggregate-prone precursor proteins. Indeed, the large pocket has dimensions of 15 × 20 × 20 Å, which can accommodate not only an extended unfolded peptide segment but also the one with secondary structures. Such a wide-open hydrophobic region may be more suitable for functioning as a chaperone than as a receptor for precise recognition of mitochondrial-targeting signals.

As described above, Tom70 not only functions as a receptor but also provides a docking site for cytosolic chaperones [40]. The N-terminal sub-domain of yeast Tom70 was suggested to offer a peptide-binding groove for the C-terminal EEVD motif of Hsp70 and Hsp90, thereby contributing to docking of the chaperone–substrate complex on the mitochondrial surface [40,41]. Tom71 is a homolog of yeast Tom70 with high sequence identity and is a minor subunit of the TOM40 complex [42,43]. Recently, the X-ray structures of the complex of Tom71 and Hsp70 or Hsp90 derived C-terminal peptides containing the EEVD motif were determined at 2.15 Å and 2.0 Å resolution, respectively [44]. Tom71 in a complex with the EEVD peptides takes an 'open' structure with its N-terminal domain being swung away from the C-terminal domain. The possible substrate-binding region of Tom71 in the open structure has a dimension of 25 × 35 × 20 Å, which is more than double the size of pocket in the closed state of Tom70. It was proposed that binding of the C-terminal EEVD peptide in cytosolic Hsp70 or Hsp90 triggers the conformational change in Tom70/Tom71 that leads to significant opening of the precursor-binding pocket in the C-terminal sub-domain and bringing it closer to Hsp70 or Hsp90 [44]. Such a conformational change of Tom70/Tom71 may contribute to efficient transfer of aggregate-prone substrates from Hsp70 and Hsp90 to Tom70/Tom71.

2.4. Passage through the TOM40 channel

After recognition by the receptor subunits of the TOM40 complex, mitochondrial precursor proteins are forwarded to the Tom40 channel perhaps via Tom5. Although β-barrel pore formation of Tom40 was suggested by its assembly pathway via the β-barrel protein specific translocator, the TOB/SAM complex [5–7], secondary structure predictions [45], and single-channel recordings of the protein reconstituted into the lipid bilayer [16], the high-resolution structure of the Tom40 channel is not yet available. However, lines of evidence suggest that the inner wall of the Tom40 channel is not entirely hydrophilic, but instead contains some hydrophobic patches [14,46]. Those hydrophobic patches may well offer an optimal environment for translocating unfolded polypeptides by weak chaperone-like interactions and/or shift the conformational equilibrium to the unfolded state, thereby facilitating the efficient threading of the precursor proteins through the Tom40 channel [46,47].

After crossing the outer membrane through the Tom40 channel, the presequence of presequence-containing proteins is recognized by another receptor site called the '*trans*' site of the TOM40 complex on the IMS side [16]. The *trans* site may be comprised of the IMS-facing region of Tom40, Tom22, and Tom7 [48–51]. While Tom22 contains a distinct IMS domain, its high-resolution structure is still elusive likely due to its poor folding capacity after isolation.

3. The TIM23 complex

3.1. The TIM23 complex in the inner membrane

The TIM23 complex is the translocator in the inner membrane that mediates translocation of presequence-containing precursor proteins

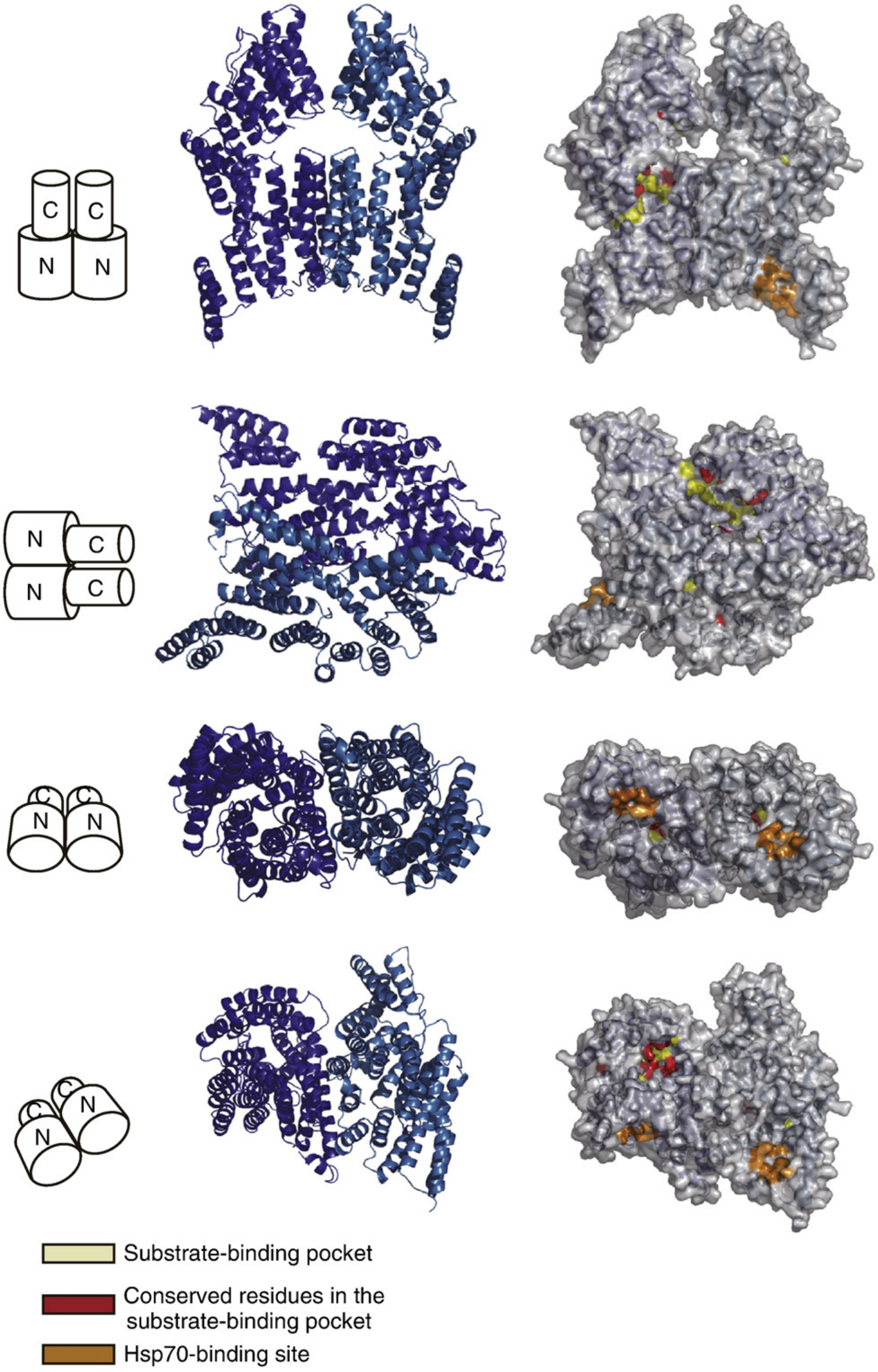

Fig. 3. The crystal structure of yeast Tom70 (2GW1). Semi-transparent molecular surface shows the structures of the yeast Tom70 receptor domain from different angles as shown in the schematic diagrams in the left. The hydrophobic residues and conserved residues in the possible substrate-binding pocket are shown in yellow and red, respectively, and the Hsp70-peptide-binding region inferred from the structure of the yeast Tom71–Hsp70 peptide complex (3FP4) in orange.

across and their insertion into the inner membrane (Fig. 1). The TIM23 complex consists of the core complex containing the three essential subunits, Tim23, Tim17, and Tim50, and multiple peripheral subunits. Tim23 exhibits a two-domain structure; the C-terminal domain contains four TM segments and constitutes a narrow protein-conducting channel, the gating of which is regulated by the membrane potential across the inner membrane and the presence of substrate presequence-containing precursor proteins [52–54]. The N-terminal domain of Tim23 is exposed to the IMS and associates with the IMS domain of Tim50 through coiled-coil interactions [55,56], which are essential for guiding the precursor protein through the Tim23 channel [55]. The most N-terminal up to 50 residues of Tim23 were proposed to insert into the outer membrane in a translocating-precursor-dependent manner [57–59], although precise roles of such outer-membrane insertion of the N-terminus of Tim23 in mitochondrial protein import still remain unclear [55].

Tim17 with four TM segments is homologous to the C-terminal membrane-embedded domain of Tim23. While it is not clear if Tim17 cooperates with Tim23 to make up a heterodimeric protein-conducting channel, Tim17 appears at least responsible for lateral protein sorting into the inner membrane [60]. Tim50 is anchored to the inner membrane by the TM segment near the N-terminus and exposes a large C-terminal domain to the IMS [61–63]. The IMS domain of Tim50 functions as a presequence receptor and receives presequence-containing proteins from the TOM40 complex [50,61]. Such transfer of the precursor proteins between the TOM40 complex and TIM23 complex is facilitated by the recently detected direct interaction of the Tim50 IMS domain with the IMS domain of Tom22 [55]. The IMS domain of Tim50 also interacts with that of Tim23 through the coiled-coil structures, which is important not only for transfer of precursor proteins from the TOM40 complex to the TIM23 complex [55,56,64], but also for regulation of the functions of the import motor components at the outlet of the Tim23 channel [55].

3.2. Tim21

Tim21, a non-essential and peripheral subunit of the TIM23 complex, associates with the TIM23 core complex consisting of Tim23, Tim17, and Tim50 [60]. Deletion of Tim21 does not give obvious defects in yeast cell growth while overexpression of Tim21 affects cell growth [59,65]. Tim21 is anchored to the inner membrane by the single TM segment, exposing the N-terminal 3 kDa domain to the matrix and the 16 kDa C-terminal domain to the IMS. Tim21 has been proposed to promote coupling of the TOM40 and Tim23 translocator complex [60,66], to switch the function of the TIM23 complex for substrate translocation across the inner membrane and lateral sorting to the inner membrane [60], and to recruit the TIM23 complex to the respiratory chain complex III [65]. However, the first and the second of the three proposed functions were questioned by other groups and are still in a hot dispute [55,59].

The crystal structure of the IMS domain of yeast Tim21 (residues 103–239) was determined at 1.6 Å resolution [67]. The Tim21 IMS domain takes a mixed α/β protein fold composed of two α-helices (α1 and α2) and eight β-strands (β1–β8). The long N-terminal helix α1 is secured to one face of the β-sheet comprised of anitparallel β-strands β1–β4 by three hydrogen bonds. The surface of the Tim21 IMS domain contains several patches of conserved positively charged residues, and such positively charged regions of Tim21 were proposed to interact with the IMS domain of Tom22 in the TOM40 complex through electrostatic interactions (Fig. 4). However, physical interactions between Tim21 and Tom22 were observed only after solubilization of mitochondria or only for high concentrations of purified recombinant components. Therefore positive evidence for their direct interaction in intact mitochondria is still missing. Indeed, the contact between the IMS domain of Tom22 and Tim23 or Tim50 in the TIM23 complex or the chase efficiency of the translocation intermediate accumulated at the TOM40 complex to the TIM23 complex was not affected by the absence of Tim21 [55].

Tim21 was also suggested to recruit respiratory chain III–IV super complexes to the TIM23 complex by direct interactions involving Qcr6 of complex III [65]. Such formation of the super complex between the TIM23 complex and the III–IV super complex could contribute to the maintenance of local ΔΨ around the TIM23 complex for efficient protein import even in the case of partial uncoupling of mitochondria. The N-terminal domain of Qcr6 is highly rich in acidic residues, and indeed, our preliminary NMR analyses revealed that the positively charged patches of Tim21 is important for direct interactions with the negatively charged N-terminal domain of Qcr6 [T. Yashiro, S. Kawano, T. Endo, unpublished results].

3.3. Motor proteins for the TIM23 complex

Mitochondrial Hsp70 (mtHsp70) in the matrix functions as an import motor for the TIM23 complex to drive vectorial translocation and active unfolding of the substrate precursor proteins in cooperation with its partner proteins, mitochondrial Hsp70-asssociated chaperone and motor (MMC) proteins [68]. Two molecules of

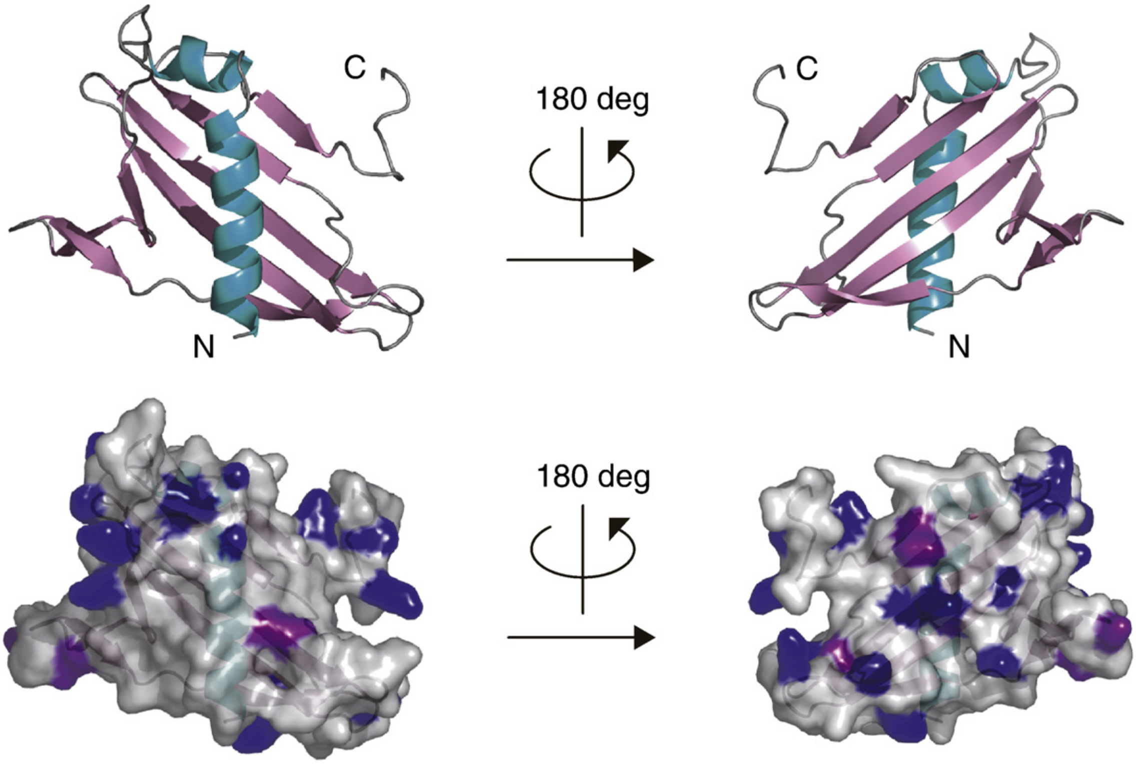

Fig. 4. The crystal structure of yeast Tim21 (2CIU). Upper panels, the ribbon model of Tim21 viewed from different angles. Lower panels, the semi-transparent molecular surface shows basic conserved residues in purple and other basic residues in dark blue.

mtHsp70 are recruited to the outlet of the TIM23 channel to become ready to bind to the unfolded segment of the substrate precursor protein [69]. Although there has been a long-standing debate on the mechanism of the active substrate-protein unfolding by the mtHsp70 import motor [68], recent evidence favors the Brownian ratchet mechanism as the simplest model to explain most of the available experimental results [70–72]. In the Brownian ratchet model, spontaneous unfolding of the mature domain of the precursor protein allows transient translocation of the unfolded segment through the import channels by Brownian motions, once the first mtHsp70 dissociates from the TIM23 complex after hydrolysis of ATP. Next, binding of the second mtHsp70 to the translocated segment in the matrix prevents backsliding and refolding, thereby leading to destabilization of the transiently unfolded species and to global unfolding of the mature domain for subsequent translocation towards the matrix.

In the reaction cycle of mtHsp70 as a chaperone ATPase, mtHsp70 requires assistance of the three essential subunits of the TIM23 complex, Tim44, Tim14/Pam18 [73–75], and Tim16/Pam16 [76,77]. Two molecules of Tim44 provide tethering sites for mtHsp70 in the ATP-bound state to grasp the unfolded translocating polypeptide segment that emerges from the outlet of the TIM23 channel [69]. Then the ATPase activity of mtHsp70 is stimulated by the J-protein Tim14/Pam18 (and Mdj2p [78]), which is recruited to Tim44 by its homologous partner protein Tim16/Pam16. In addition to those three subunits, Pam17, a non-essential subunit of the TIM23 complex, is also proposed to facilitate coupling of Tim14/Pam18 and Tim16/Pam16 with Tim44 [64,79]. Yge1/Mge1 [80–82] and Zim17/Tim15/Hep1 [83–87], which are soluble proteins in the matrix, facilitate the motor function of mtHsp70, although they are not genuine subunits of the TIM23 complex. Yge1/Mge1 promotes the ADP to ATP exchange of mtHsp70 by binding to mtHsp70 to distort the nucleotide-binding site [80–82]. Zim17/Tim15/Hep1 also binds to the nucleotide-free mtHsp70, yet its role appears mainly to be maintenance of the solubility of aggregate-prone mtHsp70 in the matrix [85,87].

3.4. Tim14/Pam18 and Tim16/Pam16

The ATPase cycle of Hsp70 is assisted by J proteins, which have a conserved J-domain with the invariant and essential His-Pro-Asp (HPD) motif to stimulate the ATPase activity of Hsp70 [88]. J proteins determine the specificity of diverse functions of Hsp70 often by interacting with specific partner proteins. In mitochondria, Tim14/Pam18, Mdj2, and Mdj1 are J proteins that function as partners for mtHsp70 (Ssc1 in yeast); Tim14/Pam18 and Mdj2 assist mtHsp70 in protein import at the TIM23 complex [73–75,78] and Mdj1 in protein folding/assembly in the matrix [89]. Tim14/Pam18 forms a stable 1:1 complex with Tim16/Pam16, which is a J-like protein homologous to Tim14/Pam18, but lacks the HPD signature motif for J proteins. Tim14/Pam18 is anchored to the inner membrane through its TM segment (residues 61–98) and exposes its N-terminal part (residues 1–60) to the IMS and the conserved C-terminal domain containing the J-domain (residues 99–168) to the matrix. While deletion of Tim14/Pam18 is lethal for the cell, deletion of the N-terminal IMS domain together with the following TM segment does not affect the growth of the mutant cells significantly [90]. Tim16/Pam16 consists of the conserved N-terminal and C-terminal domains connected by a less-conserved linker segment in between. The N-terminal domain (residues 1–24) consists of mainly hydrophobic residues and is thus responsible for the membrane association of Tim16. However, deletion of the N-terminal domain together with the linker segment does not affect the growth of the mutant cells [90].

Mokranjac et al. determined the crystal structure of the complex between the Tim14/Pam18 J-domain and Tim16/Pam16 C-terminal domain at 2.0 Å resolution [90]. Both domains take the typical folds of J-domains consisting of three helices (I–III), two of which (helices II and III) form an antiparallel hairpin connected by a linker segment containing the HPD motif in Tim14 (Fig. 5). Tim14/Pam18 and Tim16/Pam16 form a back-to-back heterodimer, in which the loops between helices II and III face opposite sides of the complex. While Tim14/Pam18 contains a positively charged region on the surface, which is characteristic of J proteins and has been proposed to play a role in the interaction with Hsp70 (Fig. 5), Tim16/Pam16 lacks such clustering of positively charged residues on the surface. The heterodimeric structure is stabilized by the N-terminal arm of Tim14/Pam18 in front of the J-domain, which embraces Tim16/Pam16 (Fig. 5, top panel). Deletion of the arm region of Tim14/Pam18 shows a deleterious effect on the function of Tim14 [90]. Interestingly *in vitro*, while Tim14/Pam18 alone can stimulate the ATPase activity of mtHsp70, Tim14/Pam18 bound to Tim16 does not exhibit such activity [90]. A likely scenario is that the Tim14/Pam18–Tim16/Pam16 complex recruited to the TIM23 core complex via Tim44 may change

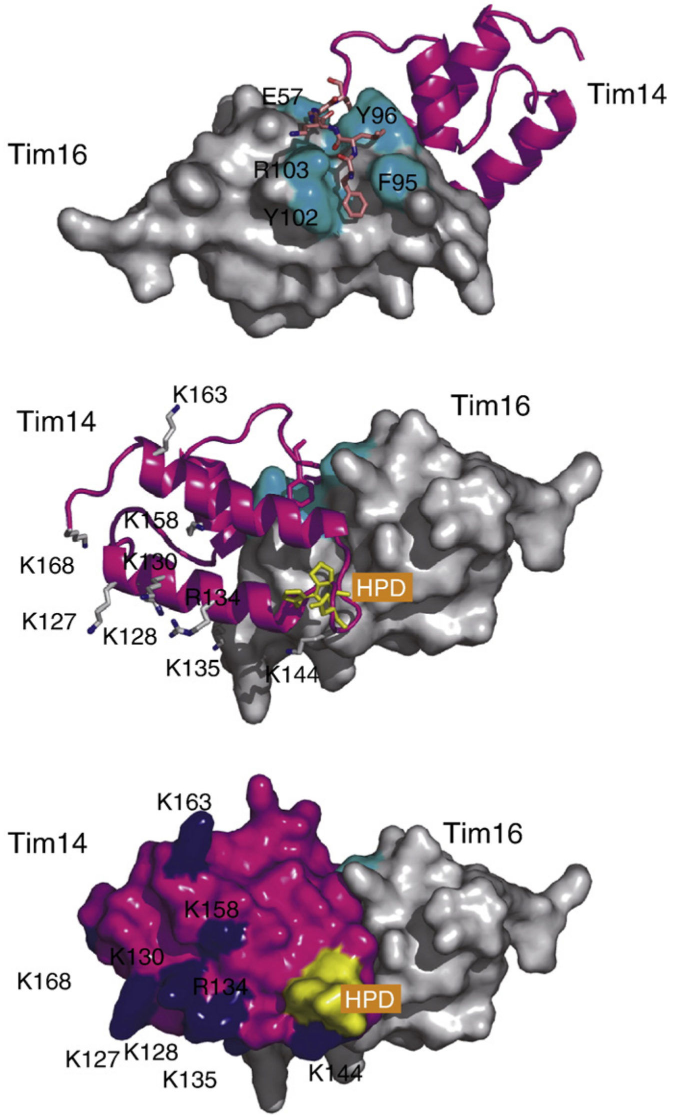

Fig. 5. The crystal structure of the yeast Tim14/Pam18–Tim16/Pam16 complex (2GUZ). Upper panel, Tim16 is shown as the surface model and Tim14 in the ribbon model. The N-terminal arm of Tim14, which embraces Tim16, is shown in the rod model (C in orange, N in dark blue, and O in red) and the Tim16 residues interacting with the arm are shown in cyan on the molecular surface. Central panel, Tim16 is shown as the surface model as in the upper panel and Tim14 in the ribbon model with the conserved HPD motif in the yellow rod model and basic residues in the gray (C) and dark blue (N) rod models. Lower panel, the surface representation of Tim16 as in the upper panel, and Tim14 in dark blue for basic residues, in yellow for the HPD motif, and in magenta for other residues.

its quaternary structure, perhaps in response to the presence of substrate polypeptide, so that Tim14/Pam18 becomes capable of stimulating the ATPase activity of mtHsp70. Indeed, loading of mitochondria with a saturating amount of precursor proteins was found to reduce crosslinking between Tim14/Pam18 and Tim16/Pam16 [59]. The resultant mtHsp70 in the ADP form can grasp the incoming precursor protein tightly, but leave the TIM23 complex, thereby allowing the substrate polypeptide to move forward by the Brownian ratchet mechanism. It is reasonable that dissociation of mtHsp70 from the TIM23 complex is regulated by not only the bound nucleotide but also binding of the peptide segment to mtHsp70 to ensure the release of only substrate-bound mtHsp70 from the TIM23 complex [91].

3.5. Tim44

Tim44 is an essential yeast protein that couples the motor functions of mtHsp70 to the Tim23 channel as described above. Tim44 behaves like a peripheral membrane protein associating with the inner membrane from the matrix side, yet a part of the Tim44 molecule is apparently accessible from the IMS side of the inner membrane [92,93]. Since Tim44 is in contact with the precursor protein in transit in the TIM23 channel [59,93,94], a part of the Tim44 molecule may perhaps dynamically penetrate from the matrix side into the Tim23 channel to some extent. Tim44 consists of two domains, the C-terminal domain of which is tightly folded and stays on the matrix side of the inner membrane. Tim44 provides an anchoring point for mtHsp70 at the exit of the Tim23 channel on the matrix side of the TIM23 complex, which ensures binding of mtHsp70 to translocating polypeptide chains in a hand-over-hand manner [95,96]. Association of two molecules of mtHsp70 with two molecules of Tim44 depends on the ADP or ATP state of mtHsp70, thereby facilitating the reaction cycle of the Brownian ratchet motor of mtHsp70 [70,97].

The crystal structures of the C-terminal domains of yeast Tim44 (residues 210–431) and human Tim44 (residues 266–452) were determined at 3.2 Å and 1.9 Å resolution, respectively [98,99]. The yeast Tim44 C-terminal domain consists of six α-helices and four β-strands. The antiparallel helices A4, A5, and A6 and the four antiparallel β-strands B1–B4 form two sides of the large pocket, respectively, the inner wall of which contains several conserved hydrophobic residues (Fig. 6). The human Tim44 C-terminal domain exhibits a similar tertiary structure containing a similar hydrophobic pocket, which, however, differs from that of yeast Tim44 in size and shape. The hydrophobic pocket in the human Tim44 is now occupied by two penta-ethylenglycol molecules [99], suggesting that the pocket may be a binding site for unfolded polypeptide segments or lipid membranes. However, this model was questioned because binding of the isolated C-terminal domain of recombinant Tim44 to cardiolipin-containing liposomes depends on the presence of helices A1 and A2, deletion of which does not disrupt the hydrophobic pocket [100].

3.6. Zim17/Tim15/Hep1

Zim17/Tim15/Hep1 is a maintenance factor for mtHsp70 and its deletion results in aggregation of mtHsp70 and defects in mtHsp70-dependent protein import into the matrix [85–87]. The NMR structure of the core domain (residues 64–159, the numbering includes the presequence) of yeast Zim17/Tim15/Hep1 was determined [87]. The Zim17/Tim15/Hep1 core domain shows an L-shaped structure, in which the two zinc-finger motifs chelating a zinc ion are located at the end of the L (Fig. 7). Mutagenesis on the basis of the NMR structure of the Zim17/Tim15/Hep1 core domain revealed that the conserved Arg, His, and Asp residues on the surface are important for the ability of Zim17/Tim15/Hep1 to suppress aggregation of mtHsp70 especially at elevated temperature (Fig. 7). Those functionally essential residues of Zim17/Tim15/Hep1 may bind to the ATPase domain and the linker between the ATPase domain and peptide-binding domain in the aggregation-prone conformer of mtHsp70, which will result in inhibition of aggregate formation [101].

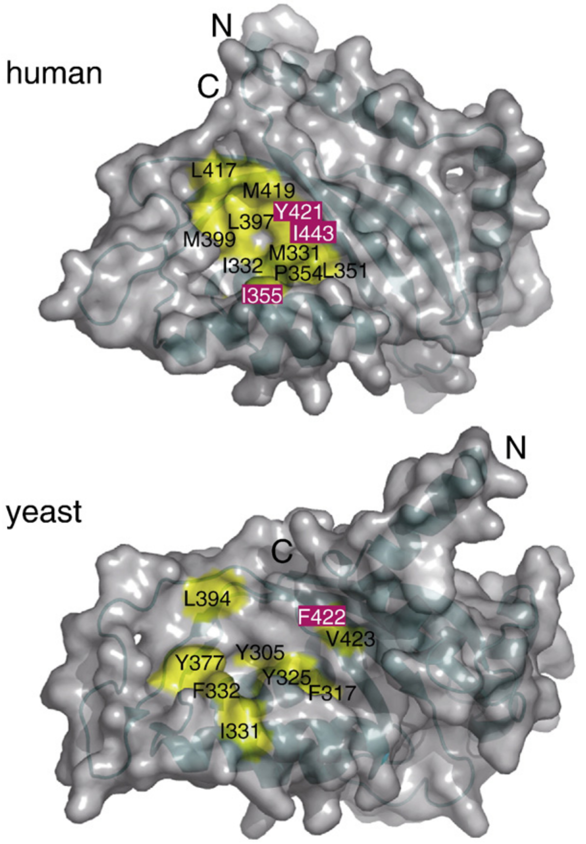

Fig. 6. The crystal structures of the C-terminal domains of human Tim44 (2CW9) and yeast Tim44 (2FXT). Hydrophobic cavity interacting with pentaethylene glycol in human Tim44 is shown in yellow, and conserved residues are indicated with letters in magenta background. The corresponding region in yeast Tim44 is shown in yellow and conserved residues with letters in magenta background [99].

3.7. Matrix processing peptidase

The presequence of precursor proteins that pass through the TIM23 channel is cleaved off by matrix processing peptidase (MPP) in the matrix [102]. MPP is a heterodimer composed of α and β subunits of ~50 kDa. Arg is generally found at position −2 from the cleavage site for MPP while +1 position in the mature part is often occupied by a bulky and hydrophobic residue such as Tyr, Leu, and Phe. Recent N-proteome analyses of yeast mitochondria showed that the N-terminal residue of a characteristic set of MPP-generated N-termini is further removed by another peptidase Icp55 [103]. The α and β subunits of MPP are homologous to the Core 2 and Core 1 subunits, respectively, of the cytochrome bc_1 complex of the mitochondrial respiratory chain. Indeed, α-MPP and β-MPPare identical to the Core 2 and Core 1 subunits in plant mitochondria, and β-MPP to the Core 2 subunit in *Neurospora crass* mitochondria [102]. In *Saccaromyces cerevisiae* and mammals, α- and β-MPP subunits are distinct from, although related to, the Core1 and Core2 proteins in the bc_1 complex.

The crystal structures of yeast MPP and its cleavage-deficient mutant (α/βE73Q MPP) complexed with presequence peptides were determined [104]. The overall folding of MPP is similar to the folds of the core proteins of the bovine bc_1 complex. The α and β subunits are related to each other by the approximate two-fold rotation, and each

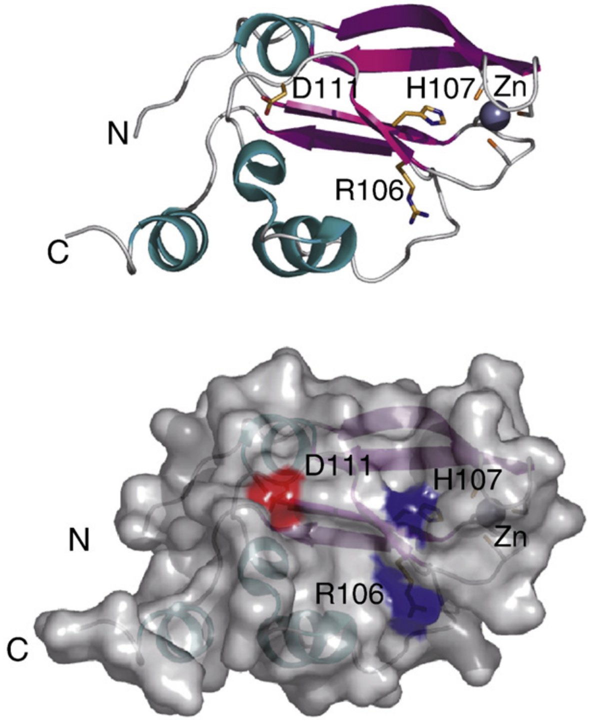

Fig. 7. The NMR structure of yeast Zim17/Tim15/Hep1 (2E2Z). Upper panel, the ribbon model of the yeast Tim15 core domain with the bound zinc ion (purple sphere) and side chains of functionally essential residues, Arg106, His107, and Asp111, in the rod model. Lower panel, the semi-transparent molecular surface shows the structure of the yeast Tim15 core domain with functionally essential residues in red (acidic Asp11) and in dark blue (basic Arg106 and His107).

subunit contains two domains with nearly identical sizes and topology (Fig. 8, upper panels). The active site of MPP is located in a large central cavity between the two subunits, which is lined with many Glu and Asp (Fig. 8, central left panel). Such acidic residues contribute to the negatively charged surface of the cavity, which is favorable for accommodating positively charged presequences. The β subunit of MPP contains Zn^{2+}, which is localized in the active-site cavity and is coordinated by β-His-70, β-His-74, β-Glu-150, and a water molecule that is within the hydrogen bonding distance to β-Glu-73. β-Glu-73 likely acts as a general base catalyst on the water molecule as was proposed for the catalytic mechanism of thermolysin [105] (Fig. 8).

Residues 7–19 of the presequence peptide (residues 2–25) of the subunit IV of cytochrome oxidase (pCoxIV) in a complex with the cleavage-deficient α/βE73Q MPP were found to take an extended conformation in the negatively charged cavity between the two subunits (Fig. 8, central right panel), which is in contrast to the helical conformation of the presequence peptide bound to the import receptor Tom20 [27]. The cleavage site for pCoxIV is between residues 17 and 18, with the cleavage-site motif comprised of basic Arg16 at position −2 and bulky Leu18 at position +1. While the carbonyl oxygen of the scissile peptide bond points toward the active-site Zn^{2+} ion, Arg16 is close to conserved βGlu-160 and βGlu-164, and Leu18 is located near conserved βPhe-77 (Fig. 8, central right panel). Unlike the pCoxIV peptide, the presequence peptide (residues 2–17) of malate dehydrogenase (pMDH) in α/βE73Q MPP was cleaved between residues 9 and 10 by the residual peptidase activity (Fig. 8, lower panels). One of the C-terminal oxygens of the cleaved pMDH is positioned as a ligand to the Zn^{2+} ion, occupying the positions of the initial water ligand (Fig. 8, central left and lower left panels). Like pCoxIV, pMDH takes an extended conformation and Arg8 at position −2 is close to βGlu160 and βAsp164 of α/βE73Q MPP.

4. Small Tim proteins

4.1. Small Tim proteins in the IMS

Protein sorting to various mitochondrial subcompartments requires cooperation of distinct translocator complexes, and the *trans* site or outlet of the protein-conducting channel of the TOM40 complex may serve as a scanning platform to which cooperating translocator components and soluble factors in the IMS can bind. Indeed, physical interactions for precursor-protein transfer were detected between the TOM40 complex and TIM23 complex in intact mitochondria irrespective of the presence of translocating-precursor proteins [55]. Small Tim proteins are also likely called for to escort aggregate-prone, often unfolded precursor proteins through the aqueous IMS to pass then from the TOM40 complex onto the TIM22 or TOB/SAM complex [106–109]. In yeast, five members of small Tim proteins have been identified; Tim9, Tim10, and Tim12 are essential for cell viability while Tim8 and Tim13 are non-essential proteins that can be deleted without obvious defects in cell growth. Tim9 and Tim10 form the $\alpha_3\beta_3$ hexameric complex in the IMS, which binds to the polytopic inner membrane-protein precursors or substrates for the TIM22 pathway emerging from the outlet of the TOM40 channel. Binding of the Tim9–Tim10 complex to its substrate proteins likely in a loop conformation prevents them from backsliding through the TOM40 channel, thereby promoting their vectorial translocation across the outer membrane [110]. The Tim9–Tim10 complex further escorts the substrate proteins through the aqueous IMS to the TIM22 complex. Then Tim9 and Tim10 rearrange their hexameric structure with Tim12, to form the membrane-bound Tim9–Tim10–Tim12 complex for transfer of the substrate proteins to the TIM22 complex. Alternatively, the Tim9–Tim10 complex transfers substrate proteins to the Tim9–Tim10–Tim12 complex, which is already associated with the TIM22 complex. The Tim9–Tim10 complex also binds to β-barrel proteins or substrates for the TOB/SAM pathway coming out of the Tom40 channel. The Tim9–Tim10 complex again escorts those β-barrel proteins to the TOB/SAM complex, where the Tim9–Tim10 complex releases its substrates. Tim8 and Tim13 also form the $\alpha_3\beta_3$ hexameric complex in the IMS, which binds to a part of the substrates for the TIM22 or TOB/SAM pathway at the outlet of the Tom40 channel. However, since Tim8 and Tim13 are dispensable for yeast cell growth, the substrate specificity for the Tim8–Tim13 complex may be overlapped by that for the Tim9–Tim10 complex.

4.2. The Tim9–Tim10 and Tim8–Tim13 complexes

The crystal structures of the human and yeast Tim9–Tim10 complexes were determined at 3.3 Å and 2.5 Å resolution, respectively [111,112]. The Tim9–Tim10 complex is composed of alternating subunits arranged into a six-bladed α-propeller structure with a central channel 10–15 Å wide (Fig. 9). Each Tim9 and Tim10 subunits form antiparallel helices that are connected by the two disulfide bridges and a 10-residue loop. Those central Cys-loops form a flat face normal to the molecular C3 symmetry axis, whereas 12 tentacle-like projections protrude from the opposite face. Since the Tim9–Tim10 complex interacts unproductively with its substrate if the inner tentacles of Tim9 are truncated, the N-terminal tentacle of Tim9 is crucial for its function [113].

The crystal structure of the yeast Tim8–Tim13 complex was also determined at 2.6 Å resolution [113]. The overall structure of the Tim8–Tim13 complex is similar to those of the Tim9–Tim10 complexes (Fig. 9). The jellyfish-like architectures of the Tim9–Tim10 and Tim8–Tim13 complexes are reminiscent of the chaperones prefoldin [114,115] and Skp [116,117]. Skp, a bacterial chaperone that guides outer-membrane proteins through the periplasmic space to the outer membrane, has three-pronged grasping forceps, each consisting of a long α-helical hairpin extension (Fig. 10). While the

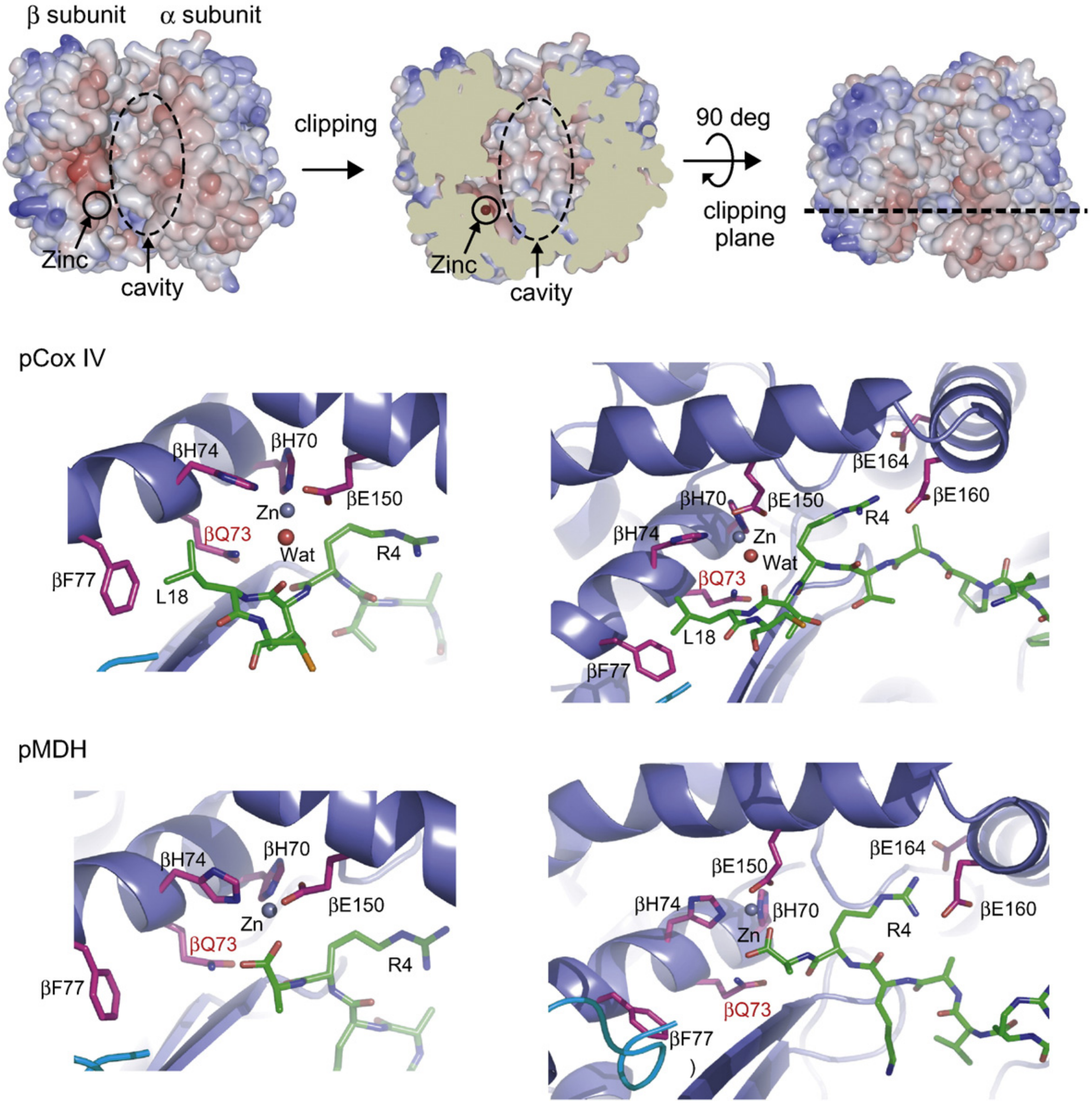

Fig. 8. The crystal structure of yeast MPP (1HR6) and its cleavage-deficient mutant (α/βE73Q MPP) in complexes with mitochondrial presequence peptides (1HR8 and 1HR9). Upper panels, electrostatic representation of MPP with positive charge in blue and negative charge in red. The upper central panel is a cutaway view of the surface representation in the upper left panel; zinc ion is shown as a red sphere. The upper right panel is surface representation in the upper left panel after the indicated rotation, showing the clipping plane for the upper central panel. Central and lower panels, structures of the active site of α/βE73Q MPP (in the ribbon model with side chains of conserved residues in the rod model, C in cyan, N in dark blue, and O in red) and bound pCoxIV peptide (central panels) and bound pMDH peptide (lower panels) (in the rod model, C in green, N in dark blue, and O in red). The zinc ion (cyan sphere) and bound water molecule (magenta sphere) are shown. The mutated residue (βGln73) is shown with red letters.

tips of the α-helical extensions are rich in positively charged residues, the inner faces of the three prongs are less charged and contain patches of hydrophobic residues, suggesting that Skp binds unfolded substrates in the prong interiors. Prefoldin, a hexameric chaperone in the cytosol of eukaryotes and archaea, forms a double β-barrel assembly with six long tentacle-like coiled coils protruding from it. The distal regions of the coiled coils expose hydrophobic patches, which are required for the multivalent interaction with unfolded proteins. The Tim9–Tim10 and Tim8–Tim13 complexes have large hydrophobic regions around the side of the barrel structures where the tentacles join (Fig. 10). Additional smaller hydrophobic patches can be found in the distal region of the tentacles. Therefore, although the tentacles of the Tim8–Tim13 and Tim9–Tim10 complexes likely provide binding sites for hydrophobic, possibly unfolded substrate proteins, it is not clear if further conformational changes are required to expose larger hydrophobic regions in the tentacles to increase affinity for the unfolded substrates.

5. The disulfide relay system

5.1. The disulfide relay system in the IMS

The IMS between the outer and inner mitochondrial membranes contains numerous, mainly small and soluble proteins. Many of those IMS proteins contain characteristic Cys-containing motifs that form internal disulfide bonds, and the IMS has a dedicated disulfide relay system to introduce disulfide bonds into those proteins. The disulfide relay system overcomes the reducing environment in the IMS due to the diffusion of reducing agents from the cytosol, likely using the respiratory chain as an oxidative electron sink.

The disulfide relay system in the mitochondrial IMS consists of two essential proteins, a disulfide carrier Tim40/Mia40 and an FAD-dependent sulfhydryl oxidase Erv1 [118–121]. Tim40/Mia40 recognizes Cys in the specific IMS targeting signals [122,123] in the newly imported substrate proteins and transfers disulfide bonds to them by

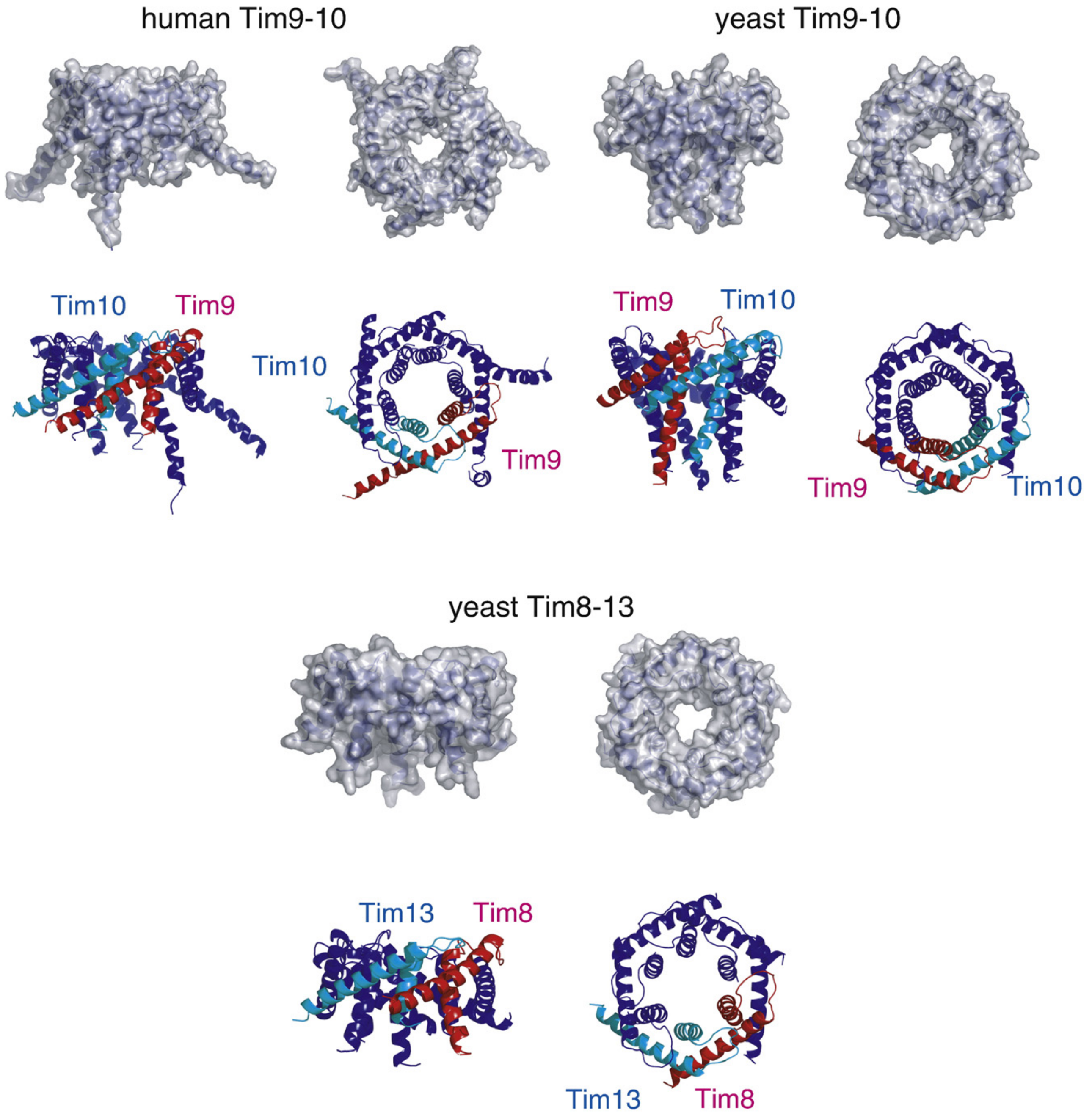

Fig. 9. The crystal structures of the human Tim9–Tim10 (2BSK), yeast Tim9–Tim10 (3DXR), and yeast Tim8–Tim13 (3CJH) complexes. Surface representation (upper panels) and the ribbon model (lower panels) for each complex viewed from different angles are shown. In the ribbon model, Tim9 and Tim10 in one adjacent pair in the hexameric complex are shown in magenta and cyan, respectively, and Tim8 and Tim13 in magenta and cyan, respectively, as well.

dithiol/disulfide exchange reactions involving mixed disulfide intermediates [120,121]. Tight folding by introduction of disulfide bonds prevents unfolding of the substrate proteins, thereby providing a driving force for vectorial translocation through the narrow pore of the TOM40 complex or at least contributing their selective retention in the IMS. After disulfide bond transfer from Tim40/Mia40 to substrate proteins, Tim40/Mia40 is reoxidized again by Erv1, which is then oxidized by electron transfer to either cytochrome *c* or molecular oxygen [124–127].

5.2. Tim40/Mia40

Yeast Tim40/Mia40 has a long N-terminal region and is anchored to the inner membrane by the N-terminal TM segment, exposing the conserved C-terminal region to the IMS [118,128]. On the other hand, Tim40/Mia40 in animals and plants has only a short N-terminal region lacking the TM segment and is soluble in the IMS [129]. Yeast Tim40/Mia40 lacking the TM segment and soluble human Tim40/Mia40 are fully functional in yeast cells [118,130]. The conserved C-terminal domain of Tim40/Mia40 contains three conserved disulfide bonds, the first of which as the CPC motif is involved in the disulfide bond transfer to substrate proteins.

High-resolution structures were recently determined for the C-terminal core domains of human MIA40 (residues 1–146) by NMR [131] and yeast Tim40/Mia40 (residues 284–365) by X-ray diffraction analyses at 3.0 Å resolution [132]. Both human MIA40 and yeast Tim40/Mia40 core domains consist of a long N-terminal loop followed by two 13-residue α-helices (Fig. 11). Those two helices are

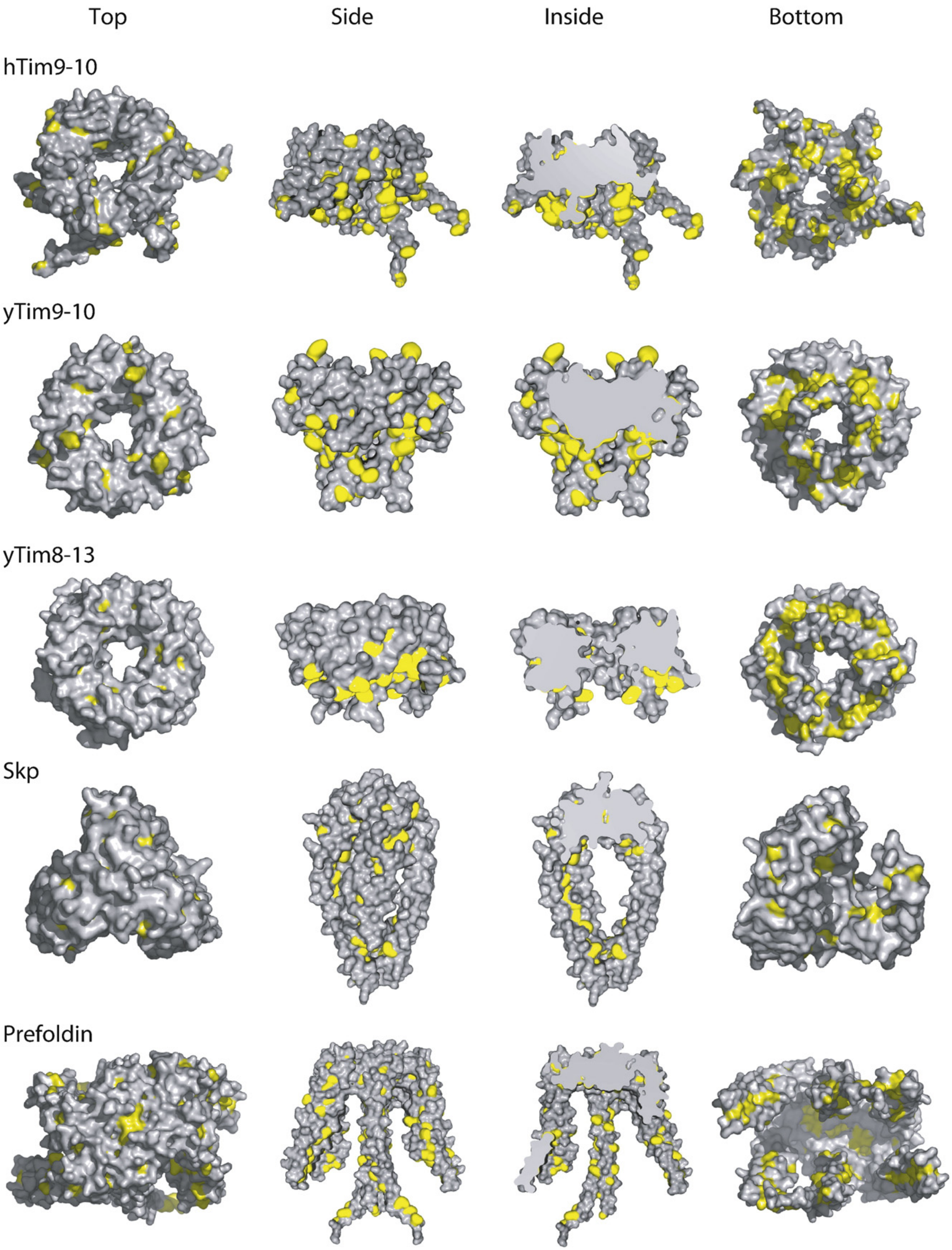

Fig. 10. Comparison of the crystal structures of the Tim9–Tim10 complex, Tim8–Tim13 complex, Skp, and prefoldin. Top view (left panels), side view (second left panels), longitudinal section (second right panels), and bottom view (right panels) of the crystal structures of the human Tim9–Tim10 complex (hTim9-10, 2BSK), yeast Tim9–Tim10 complex (yTim9-10, 3DXR), yeast Tim8–Tim13 complex (yTim8-13, 3CJH), *E. coli* Skp (1SG2), and prefoldin from *Methanothermobacter thermautotrophicus* (1FXK) are shown in the semi-transparent surface model with hydrophobic residues in yellow.

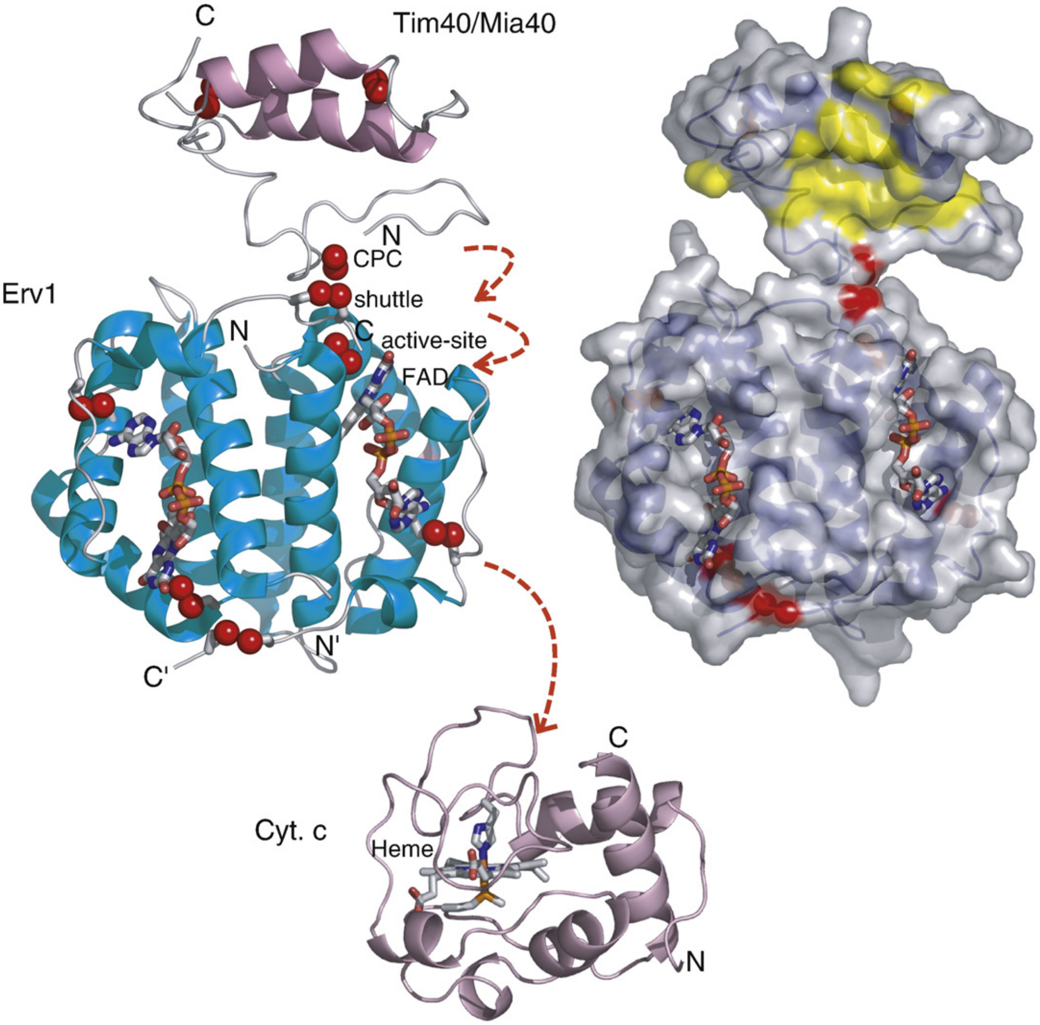

Fig. 11. The disulfide relay system consisting of Tim40 and Erv1 with cytochrome *c*. Left panels, the yeast Tim40/Mia40 core domain (2ZXT), dimeric plant Erv1 core domain (3HJ3), and yeast cytochrome *c* (Cyt. c, 3CX5) are shown in the ribbon model. The C-terminus of the plant Erv1 core domain is extended by five and seven residues in each subunit in arbitrary conformations. The sulfur atoms of Cys residues are shown in the red sphere, and FAD in Erv1 and heme in cytochrome *c* are shown in the rod model (C in gray, O in red, and N in dark blue). CPC, the CPC motif mediating the disulfide bond transfer in Tim40; shuttle, the shuttle disulfide; active-site, the active-site disulfide. The flow of electron is shown with red broken arrows. Right panels, the yeast Tim40/Mia40 core domain and the plant Erv1 core domain viewed as in the left panels are shown in the semi-transparent surface model. Hydrophobic residues in the substrate-binding site of Tim40/Mia40 are shown in yellow, and Cys residues in Tim40/Mia40 and Erv1 in red.

connected by the second and third disulfide bonds to form an antiparallel α-helical hairpin. Interestingly, in the crystal structure of the Tim40/Mia40 core domain fused to maltose binding protein (MBP), the 11-residue linker segment between MBP and the Tim40/Mia40 core is accommodated, partly forming a helical structure, in the relatively wide hydrophobic concave region on the surface of the fruit-dish like Tim40/Mia40 core domain [132]. The linker segment may well mimic a substrate peptide segment to be recognized by Tim40/Mia40. Indeed, when we replaced the linker segment with the possible IMS targeting signal derived from the authentic substrate Tim9 [132], similar binding to the hydrophobic region was observed [S. Kawano, N. Watanabe, T. Endo, unpublished results]. Substitution of hydrophilic, not hydrophobic, amino acids for the residues constituting the hydrophobic region led to functional defects of Tim40 reflected in the temperature-sensitive cell growth defects [132].

5.3. Erv1

While Tim40/Mia40 mediates disulfide bond formation in substrate proteins, Erv1 reoxidizes reduced Tim40/Mia40 for the next round of the Tim40/Mia40-mediated disulfide transfer [120,121]. Erv1, which is called ALR (*A*ugmenter of *L*iver *R*egeneration) in mammals, is a soluble protein in the IMS and forms a homodimer. High-resolution crystal structures are available for *A. thaliana* Erv1 (AtErv1, residues 71–191) [133], rat ALR (residues 1–125) [134], and yeast Erv1 (residues 78–189) [S. Kawano, N. Watanabe, T. Endo, unpublished results] at 2.5 Å, 1.6 Å and 2.0 Å resolution, respectively. These enzymes form head-to-tail homodimers, each subunit consisting of the core domain of ~100 amino-acid residues and flanking flexible segments [135]. For example, in the crystal structures of plant Erv1 (residues 71–191) and rat ALR (residues 1–125), the C-terminal region (residues 174–191) and N-terminal region (residues 1–12), respectively, are disordered. The tightly folded core domains of Erv1 from different organisms consist of five α-helices, four of which form a bundle that accommodates the isoalloxazine ring of FAD (Fig. 11). The core domain contains the 'active-site' disulfide, which is juxtaposed with the FAD isoalloxazine ring and is supposed to transfer electrons to flavin. Erv1 contains another disulfide essential for functions *in vivo*, which is referred to as the 'shuttle' disulfide, in the flexible segment N-terminal (yeast and mammalian Erv1) or C-terminal (plant Erv1) to the core domain [136]. While being in close proximity to the FAD isoalloxazine ring, the active-site Cys pair is not accessible to the authentic substrate Tim40/

Mia40. Instead, the shuttle disulfide may receive electrons from Tim40/Mia40 by forming a transient mixed disulfide intermediate, and then transfer electrons to the active-site disulfide in the other subunit of the homodimer complex [10] (Fig. 11). Subsequently, reduced FAD transfers electrons to an appropriate electron acceptor including cytochrome *c* and molecular oxygen (Fig. 11).

6. Perspective

Although an increasing number of high-resolution structures of the soluble domains/proteins of the components constituting the mitochondrial protein import system have become available, many of the components are still on the queue for every endeavor to determine their X-ray and/or NMR structures. More seriously, no high-resolution structures are available for membrane-embedded parts including protein-conducting channels of the import machineries. Although import channel proteins such as Tom40 [18], Tim23 [52], Tim22 [137], and Sam50/Tob55 [138] can be expressed in *E. coli* cells and refolded into functional structures in the lipid bilayer, they appear suitable for merely single-channel recordings or single-particle analyses in electron microscopy probably due to difficulty in getting enough materials for crystallization. The functional entire TOM40 complex can be reportedly obtained in large amounts from *N. crassa* cells [14], yet they may still have problems in forming well-ordered crystals, as well. Therefore, in spite of the on-going advancement of the methodology for two-dimensional and three-dimensional membrane-protein crystallization and NMR structural determination, we are still not certain when the integral membrane components of the mitochondrial import system are subdued for structural determination. Nevertheless, in view of the fruitful outcome of the revealed high-resolution structures of bacterial Sec translocon channels [139–141], we still hope that a mist will be finally lifted from the stunning beauty of the entire structures of the mitochondrial protein import machineries in the not too distant future.

Acknowledgements

We thank members of the Endo laboratory for discussions and comments. The authors are supported by Grants-in Aid for Scientific Research from the Ministry of Education, Culture, Sports, Science and Technology of Japan (MEXT).

References

[1] C.M. Koehler, New developments in mitochondrial assembly, Annu. Rev. Cell Dev. Biol. 20 (2004) 309–335.
[2] W. Neupert, J.M. Hermann, Translocation of proteins into mitochondria, Annu. Rev. Biochem. 76 (2007) 723–749.
[3] T. Endo, K. Yamano, Multiple pathways for mitochondrial protein traffic, Biol. Chem. 390 (2009) 723–730.
[4] A. Chacinska, C.M. Koehler, D. Milenkovic, T. Lithgow, N. Pfanner, Importing mitochondrial proteins: machineries and mechanisms, Cell 138 (2009) 628–644.
[5] S.A. Paschen, W. Neupert, D. Rapaport, Biogenesis of beta-barrel membrane proteins of mitochondria, Trends Biochem. Sci. 30 (2005) 575–582.
[6] T. Becker, F.-N. Vögtle, D. Stojanovski, C. Meisinger, Sorting and assembly of mitochondrial outer membrane proteins, Biochim. Biophys. Acta 1888 (2008) 557–563.
[7] T. Endo, K. Yamano, Transport of proteins across or into the mitochondrial outer membrane, Biochim. Biophys. Acta 1803 (2010) 706–714.
[8] J. Riemer, N. Bulleid, J.M. Herrmann, Disulfide formation in the ER and mitochondria: two solutions to a common process, Science 324 (2009) 1284–1287.
[9] C.M. Koehler, H.L. Tienson, Redox regulation of protein folding in the mitochondrial intermembrane space, Biochim. Biophys. Acta 1793 (2009) 138–145.
[10] M. Duponte, K. Hell, Disulphide bond formation in the intermembrane space of mitochondria, J. Biochem. 146 (2009) 599–608.
[11] T. Endo, K. Yamano, S. Kawano, Structural basis for the disulfide relay system in the mitochondrial intermembrane space, Antioxid. Redox Signal. (2010), doi:10.1089/ars.2010.3099.
[12] D. Roise, G. Schatz, Mitochondrial presequences, J. Biol. Chem. 263 (1988) 4509–4511.
[13] T. Endo, D. Kohda, Functions of outer membrane receptors in mitochondrial protein import, Biochim. Biophys. Acta 1592 (2002) 3–14.
[14] K.P. Künkele, S. Heins, M. Dembowski, F.E. Nargang, R. Benz, M. Thieffry, J. Walz, R. Lill, S. Nussberger, W. Neupert, The preprotein translocation channel of the outer membrane of mitochondria, Cell 93 (1998) 1009–1019.
[15] U. Ahting, C. Thun, R. Hegerl, D. Typke, F.E. Nargang, W. Neupert, S. Nussberger, The TOM core complex, the general protein import pore of the outer membrane of mitochondria, J. Cell Biol. 147 (1999) 959–968.
[16] K. Model, T. Prinz, T. Ruiz, M. Radermacher, T. Krimmer, W. Kühlbrandt, N. Pfanner, C. Meisinger, Protein translocase of the outer mitochondrial membrane: role of import receptors in the structural organization of the TOM complex, J. Mol. Biol. 316 (2002) 657–666.
[17] K. Model, C. Meisinger, W. Kühlbrandt, Cryo-electron microscopy structure of a yeast mitochondrial preprotein translocase, J. Mol. Biol. 383 (2008) 1049–1057.
[18] K. Hill, K. Model, M.T. Ryan, K. Dietmeier, F. Martin, R. Wagner, N. Pfanner, Tom40 forms the hydrophilic channel of the mitochondrial import pore for preproteins, Nature 395 (1998) 516–521.
[19] S. van Wilpe, M.T. Ryan, K. Hill, A.C. Maarse, C. Meisinger, J. Brix, P.J. Dekker, M. Moczko, R. Wagner, M. Meijer, B. Guiard, A. Hönlinger, N. Pfanner, Tom22 is a multifunctional organizer of the mitochondrial preprotein translocase, Nature 401 (1999) 485–489.
[20] T. Söllner, G. Griffiths, R. Pfaller, N. Pfanner, W. Neupert, Mom19, an import receptor for mitochondrial precursor proteins, Cell 59 (1989) 1061–1070.
[21] M. Moczko, F. Gärtner, N. Pfanner, The protein import receptor MOM19 of yeast mitochondria, FEBS Lett. 326 (1993) 251–254.
[22] L. Ramage, T. Junne, K. Hahne, T. Lithgow, G. Schatz, Functional cooperation of mitochondrial protein import receptors in yeast, EMBO J. 12 (1993) 4115–4123.
[23] A.J. Perry, J.M. Hulett, V.A. Likić, T. Lithgow, P.R. Gooley, Convergent evolution of receptors for protein import into mitochondria, Curr. Biol. 16 (2006) 221–229.
[24] G. von Heijne, Mitochondrial targeting sequences may form amphiphilic helices, EMBO J. 5 (1986) 1335–1342.
[25] D. Roise, S.J. Horvath, J.M. Tomich, J.H. Richards, G. Schatz, A chemically synthesized pre-sequence of an imported mitochondrial protein can form an amphiphilic helix and perturb natural and artificial phospholipid bilayers, EMBO J. 5 (1986) 1327–1334.
[26] T. Endo, I. Shimada, D. Roise, F. Inagaki, N-terminal half of a mitochondrial presequence peptide takes a helical conformation when bound to dodecylphosphocholine micelles: a proton nuclear magnetic resonance study, J. Biochem. 106 (1989) 396–400.
[27] Y. Abe, T. Shodai, T. Muto, K. Mihara, H. Torii, S. Nishikawa, T. Endo, D. Kohda, Structural basis of presequence recognition by the mitochondrial protein import receptor Tom20, Cell 100 (2000) 551–560.
[28] T. Muto, T. Obita, Y. Abe, T. Shodai, T. Endo, D. Kohda, NMR identification of the Tom20 binding segment in mitochondrial presequences, J. Mol. Biol. 306 (2001) 137–143.
[29] A. Mukhopadhyay, C.-S. Yang, H. Weiner, Binding of mitochondrial leader sequences to Tom20 assessed using a bacterial two-hybrid system shows that hydrophobic interactions are essential and that some mutated leaders that do not bind Tom20 can still be imported, Protein Sci. 15 (2006) 2739–2748.
[30] R. Pfaller, N. Pfanner, W. Neupert, Mitochondrial protein import, bypass of proteinaceous surface receptors can occur with low specificity and efficiency, J. Biol. Chem. 264 (1989) 34–39.
[31] T. Lithgow, G. Schatz, Import of the cytochrome oxidase subunit Va precursor into yeast mitochondria is mediated by the outer membrane receptor Mas20p, J. Biol. Chem. 270 (1995) 14267–14269.
[32] T. Saitoh, M. Igura, T. Obita, T. Ose, R. Kojima, K. Maenaka, T. Endo, D. Kohda, Tom20 recognizes mitochondrial presequences through dynamic equilibrium among multiple bound states, EMBO J. 26 (2007) 4777–4787.
[33] N. Pfanner, Protein sorting: recognizing mitochondrial presequences, Curr. Biol. 10 (2000) R412–R415.
[34] K. Dietmeier, A. Hönlinger, U. Bömer, P.J. Dekker, C. Eckerskorn, F. Lottspeich, M. Kübrich, N. Pfanner, Tom5 functionally links mitochondrial preprotein receptors to the general import pore, Nature 388 (1997) 195–200.
[35] K. Yamano, Y. Yatsukawa, M. Esaki, A.E.A. Hobbs, R.E. Jensen, T. Endo, Tom20 and Tom22 share the common signal recognition pathway in mitochondrial protein import, J. Biol. Chem. 283 (2008) 3799–3807.
[36] T. Söllner, R. Pfaller, G. Griffiths, N. Pfanner, W. Neupert, A mitochondrial import receptor for the ADP/ATP carrier, Cell 62 (1990) 107–115.
[37] V. Hines, A. Brandt, G. Griffiths, H. Horstmann, H. Brütsch, G. Schatz, Protein import into yeast mitochondria is accelerated by the outer membrane protein MAS70, EMBO J. 9 (1990) 3191–3200.
[38] H.F. Steger, T. Söllner, M. Kiebler, K.A. Dietmeier, R. Pfaller, K.S. Trülzsch, M. Tropschug, W. Neupert, N. Pfanner, Import of ADP/ATP carrier into mitochondria: two receptors act in parallel, J. Cell Biol. 111 (1990) 2353–2363.
[39] H. Yamamoto, K. Fukui, H. Takahashi, S. Kitamura, T. Shiota, K. Terao, M. Uchida, M. Esaki, S. Nishikawa, T. Yoshihisa, K. Yamano, T. Endo, Roles of Tom70 in import of presequence-containing mitochondrial proteins, J. Biol. Chem. 284 (2009) 31635–31646.
[40] J.C. Young, N.J. Hoogenraad, F.U. Hartl, Molecular chaperones Hsp90 and Hsp70 deliver preproteins to the mitochondrial import receptor Tom70, Cell 112 (2003) 41–50.
[41] Y. Wu, B. Sha, Crystal structure of yeast mitochondrial outer membrane translocon member Tom70p, Nat. Struct. Mol. Biol. 13 (2006) 589–593.
[42] U. Bömer, N. Pfanner, K. Dietmeier, Identification of a third yeast mitochondrial Tom protein with tetratrico peptide repeats, FEBS Lett. 382 (1996) 153–158.

[43] J. Schlossmann, R. Lill, W. Neupert, D.A. Court, Tom71, a novel homologue of the mitochondrial preprotein receptor Tom70, J. Biol. Chem. 271 (1996) 17890–17895.

[44] J. Li, X. Qian, J. Hu, B. Sha, Molecular chaperone Hsp70/Hsp90 prepares the mitochondrial outer membrane translocon receptor Tom71 for preprotein loading, J. Biol. Chem. 284 (2009) 23852–23859.

[45] L. Becker, M. Bannwarth, C. Meisinger, K. Hill, K. Model, T. Krimmer, R. Casadio, K. N. Truscott, G.E. Schulz, N. Pfanner, R. Wagner, Preprotein translocase of the outer mitochondrial membrane: reconstituted Tom40 forms a characteristic TOM pore, J. Mol. Biol. 353 (2005) 1011–1020.

[46] M. Esaki, T. Kanamori, S. Nishikawa, I. Shin, P.G. Schultz, T. Endo, Tom40 protein import channel binds to non-native proteins and prevents their aggregation, Nat. Struct. Biol. 10 (2003) 988–994.

[47] T. Stan, U. Ahting, M. Dembowski, K.-P. Künkele, S. Nussberger, W. Neupert, D. Rapaport, Recognition of preproteins by the isolated TOM complex of mitochondria, EMBO J. 19 (2000) 4895–4902.

[48] D. Rapaport, W. Neupert, R. Lill, Mitochondrial protein import. Tom40 plays a major role in targeting and translocation of preproteins by forming a specific binding site for the presequence, J. Biol. Chem. 272 (1997) 18725–18731.

[49] M. Moczko, U. Bömer, M. Kübrich, N. Zufall, A. Hönlinger, N. Pfanner, The intermembrane space domain of mitochondrial Tom22 functions as a trans binding site for preproteins with N-terminal targeting sequences, Mol. Cell. Biol. 17 (1997) 6574–6584.

[50] T. Kanamori, S. Nishikawa, M. Nakai, I. Shin, P.G. Schultz, T. Endo, Uncoupling of transfer of the presequence and unfolding of the mature domain in precursor translocation across the mitochondrial outer membrane, Proc. Natl. Acad. Sci. USA 96 (1999) 3634–3639.

[51] M. Esaki, H. Shimizu, T. Ono, H. Yamamoto, T. Kanamori, S. Nishikawa, T. Endo, Mitochondrial protein import: requirement of the presequence elements and TOM components for precursor binding to the TOM complex, J. Biol. Chem. 279 (2004) 45701–45707.

[52] K.N. Truscott, P. Kovermann, A. Geissler, A. Merlin, M. Meijer, A.J.M. Driessen, J. Rassow, N. Pfanner, R. Wagner, A presequence- and voltage-sensitive channel of the mitochondrial preprotein translocase formed by Tim23, Nat. Struct. Biol. 8 (2001) 1074–1082.

[53] M. Meinecke, R. Wagner, P. Kovermann, B. Guiard, D.U. Mick, D.P. Hutu, W. Voos, K.N. Truscott, A. Chacinska, N. Pfanner, P. Rehling, Tim50 maintains the permeability barrier of the mitochondrial inner membrane, Science 312 (2006) 1523–1526.

[54] N.N. Alder, R.E. Jensen, A.E. Johnson, Fluorescence mapping of mitochondrial TIM23 complex reveals a water-facing substrate-interacting helix surface, Cell 134 (2008) 439–450.

[55] Y. Tamura, Y. Harada, T. Shiota, K. Yamano, K. Watanabe, M. Yokota, H. Yamamoto, H. Sesaki, T. Endo, Tim23–Tim50 pair coordinates functions of translocators and motor proteins in mitochondrial protein import, J. Cell Biol. 184 (2009) 129–141.

[56] D. Mokranjac, M. Sichting, D. Popov-Čeleketić, K. Mapa, L. Gevorkyan-Airapetov, K. Zohary, K. Hell, A. Azem, W. Neupert, Role of Tim50 in the transfer of precursor proteins from the outer to the inner membrane in mitochondria, Mol. Biol. Cell 20 (2009) 1400–1407.

[57] M. Donzeau, K. Kaldi, A. Adam, S. Paschen, G. Wanner, B. Guiard, M.F. Bauer, W. Neupert, M. Brunner, Tim23 links the inner and outer mitochondrial membranes, Cell 101 (2000) 401–412.

[58] A.S. Reichert, W. Neupert, Contact sites between the outer and inner membrane of mitochondria: role in protein transport, Biochim. Biophys. Acta 1592 (2002) 41–49.

[59] D. Popov-Celeketic, K. Mapa, W. Neupert, D. Mokranjac, Active remodelling of the TIM23 complex during translocation of preproteins into mitochondria, EMBO J. 27 (2008) 1469–1480.

[60] A. Chacinska, M. Lind, A.E. Frazier, J. Dudek, C. Meisinger, A. Geissler, A. Sickmann, H.E. Meyer, K.N. Truscott, B. Guiard, N. Pfanner, P. Rehling, Mitochondrial presequence translocase: switching between TOM tethering and motor recruitment involves Tim21 and Tim17, Cell 120 (2005) 817–829.

[61] H. Yamamoto, M. Esaki, T. Kanamori, Y. Tamura, S. Nishikawa, T. Endo, Tim50 is a subunit of the TIM23 complex that links protein translocation across the outer and inner mitochondrial membranes, Cell 111 (2002) 519–528.

[62] A. Geissler, A. Chacinska, K.N. Truscott, N. Wiedemann, K. Brandner, A. Sickmann, H.E. Meyer, C. Meisinger, N. Pfanner, P. Rehling, The mitochondrial presequence translocase: an essential role of Tim50 in directing preproteins to the import channel, Cell 111 (2002) 507–518.

[63] D. Mokranjac, S.A. Paschen, C. Kozany, H. Prokisch, S.C. Hoppins, F.E. Nargang, W. Neupert, K. Hell, Tim50, a novel component of the TIM23 preprotein translocase of mitochondria, EMBO J. 22 (2003) 816–825.

[64] L. Gevorkyan-Airapetov, K. Zohary, D. Popov-Čeleketić, K. Mapa, K. Hell, W. Neupert, A. Azem, D. Mokranjac, Interaction of Tim23 with Tim50 is essential for protein translocation by the mitochondrial TIM23 complex, J. Biol. Chem. 284 (2009) 4865–4872.

[65] M. van der Laan, N. Wiedemann, D.U. Mick, B. Guiard, P. Rehling, N. Pfanner, A role for Tim21 in membrane-potential-dependent preprotein sorting in mitochondria, Curr. Biol. 16 (2006) 2271–2276.

[66] D. Mokranjac, D. Popov-Celeketic, K. Hell, W. Neupert, Role of Tim21 in mitochondrial translocation contact sites, J. Biol. Chem. 280 (2005) 23437–23440.

[67] R. Albrecht, P. Rehling, A. Chacinska, J. Brix, S.A. Cadamuro, R. Volkmer, B. Guiard, N. Pfanner, K. Zeth, The Tim21 binding domain connects the preprotein translocases of both mitochondrial membranes, EMBO Rep. 7 (2006) 1233–1238.

[68] W. Neupert, M. Brunner, The protein import motor of mitochondria, Nat. Rev. Mol. Cell Biol. 3 (2002) 555–565.

[69] F. Moro, C. Sirrenberg, H.C. Schneider, W. Neupert, M. Brunner, The TIM17.23 preprotein translocase of mitochondria: composition and function in protein transport into the matrix, EMBO J. 18 (1999) 3667–3675.

[70] Q. Liu, P. D'Silva, W. Walter, J. Marszalek, E.A. Craig, Regulated cycling of mitochondrial Hsp70 at the protein import channel, Science 300 (2003) 139–141.

[71] K. Okamoto, A. Brinker, S.A. Paschen, I. Moarefi, M. Hayer-Hartl, W. Neupert, M. Brunner, The protein import motor of mitochondria: a targeted molecular ratchet driving unfolding and translocation, EMBO J. 15 (2002) 3659–3671.

[72] K. Yamano, M. Kuroyanagi-Hasegawa, M. Esaki, M. Yokota, T. Endo, Step-size analyses of the mitochondrial Hsp70 import motor reveal the Brownian ratchet in operation, J. Biol. Chem. 283 (2008) 27325–27332.

[73] D. Mokranjac, M. Sichting, W. Neupert, K. Hell, Tim14, a novel key component of the import motor of the TIM23 protein translocase of mitochondria, EMBO J. 22 (2003) 4945–4956.

[74] K.N. Truscott, W. Voos, A.E. Frazier, M. Lind, Y. Li, A. Geissler, J. Dudek, H. Muller, A. Sickmann, H.E. Meyer, C. Meisinger, B. Guiard, P. Rehling, N. Pfanner, A J-protein is an essential subunit of the presequence translocase-associated protein import motor of mitochondria, J. Cell Biol. 163 (2003) 707–713.

[75] P.D. D'Silva, B. Schilke, W. Walter, A. Andrew, E.A. Craig, J protein cochaperone of the mitochondrial inner membrane required for protein import into the mitochondrial matrix, Proc. Natl. Acad. Sci. USA 100 (2003) 13839–13844.

[76] C. Kozany, D. Mokranjac, M. Sichting, W. Neupert, K. Hell, The J domain-related cochaperone Tim16 is a constituent of the mitochondrial TIM23 preprotein translocase, Nat. Struct. Mol. Biol. 11 (2004) 234–241.

[77] A.E. Frazier, J. Dudek, B. Guiard, W. Voos, Y. Li, M. Lind, C. Meisinger, A. Geissler, A. Sickmann, H.E. Meyer, V. Bilanchone, M.G. Cumsky, K.N. Truscott, N. Pfanner, P. Rehling, Pam16 has an essential role in the mitochondrial protein import motor, Nat. Struct. Mol. Biol. 11 (2004) 226–233.

[78] D. Mokranjac, M. Sichting, D. Popov-Celeketić, A. Berg, K. Hell, W. Neupert, The import motor of the yeast mitochondrial TIM23 preprotein translocase contains two different J proteins, Tim14 and Mdj2, J. Biol. Chem. 280 (2005) 31608–31614.

[79] M. van der Laan, A. Chacinska, M. Lind, I. Perschil, A. Sickmann, H.E. Meyer, B. Guiard, C. Meisinger, N. Pfanner, P. Rehling, Pam17 is required for architecture and translocation activity of the mitochondrial protein import motor, Mol. Cell. Biol. 25 (2005) 7449–7458.

[80] L. Bolliger, O. Deloche, B.S. Glick, C. Georgopoulos, P. Jenö, N. Kronidou, M. Horst, N. Morishima, G. Schatz, A mitochondrial homolog of bacterial GrpE interacts with mitochondrial hsp70 and is essential for viability, EMBO J. 13 (1994) 1998–2006.

[81] M. Nakai, Y. Kato, E. Ikeda, A. Toh-e, T. Endo, Yge1p, a eukaryotic GrpE homolog, is localized in the mitochondrial matrix and interacts with mitochondrial hsp70, Biochem. Biophys. Res. Commun. 200 (1994) 435–442.

[82] S. Laloraya, B.D. Gambill, E.A. Craig, A role for a eukaryotic GrpE-related protein, Mge1p, in protein translocation, Proc. Natl. Acad. Sci. U.S.A. 91 (1994) 6481–6485.

[83] L. Burri, K. Vascotto, S. Fredersdorf, R. Tiedt, M.N. Hall, T. Lithgow, Zim17, a novel zinc finger protein essential for protein import into mitochondria, J. Biol. Chem. 279 (2004) 50243–50249.

[84] H. Yamamoto, T. Momose, Y. Yatsukawa, C. Ohshima, D. Ishikawa, T. Sato, Y. Tamura, Y. Ohwa, T. Endo, Identification of a novel member of yeast mitochondrial Hsp70-associated motor and chaperone proteins that facilitates protein translocation across the inner membrane, FEBS Lett. 579 (2005) 507–511.

[85] M. Sichting, D. Mokranjac, A. Azem, W. Neupert, K. Hell, Maintenance of structure and function of mitochondrial Hsp70 chaperones requires the chaperone Hep1, EMBO J. 24 (2005) 1046–1056.

[86] L.K. Sanjuan-Szklarz, B. Guiard, M. Rissler, N. Wiedemann, V. Kozjak, M. van der Laan, C. Lohaus, K. Marcus, H.E. Meyer, A. Chacinska, N. Pfanner, C. Meisinger, Inactivation of the mitochondrial heat shock protein Zim17 leads to aggregation of matrix Hsp70s followed by pleiotropic effects on morphology and protein biogenesis, J. Mol. Biol. 351 (2005) 206–218.

[87] T. Momose, C. Ohshima, M. Maeda, T. Endo, Structural basis of functional cooperation of Tim15/Zim17 with yeast mitochondrial Hsp70, EMBO Rep. 8 (2007) 664–670.

[88] B. Bukau, A.L. Horwich, The Hsp70 and Hsp60 chaperone machines, Cell 92 (1998) 351–366.

[89] N. Rowley, C. Prip-Buus, B. Westermann, C. Brown, E. Schwarz, B. Barrell, W. Neupert, Mdj1p, a novel chaperone of the DnaJ family, is involved in mitochondrial biogenesis and protein folding, Cell 77 (1994) 249–259.

[90] D. Mokranjac, G. Bourenkov, K. Hell, W. Neupert, M. Groll, Structure and function of Tim14 and Tim16, the J and J-like components of the mitochondrial protein import motor, EMBO J. 25 (2006) 4675–4685.

[91] K. Mapa, M. Sikor, V. Kudryavtsev, K. Waegemann, S. Kalinin, C.A. Seidel, W. Neupert, D.C. Lamb, D. Mokranjac, The conformational dynamics of the mitochondrial Hsp70 chaperone, Mol. Cell 38 (2010) 89–100.

[92] P.E. Scherer, U.C. Manning-Krieg, P. Jenö, G. Schatz, M. Horst, Identification of a 45-kDa protein at the protein import site of the yeast mitochondrial inner membrane, Proc. Natl. Acad. Sci. U.S.A. 89 (1992) 11930–11934.

[93] T. Kanamori, S. Noshikawa, I. Shin, P.G. Schultz, T. Endo, Probing the environment along the protein import pathways in yeast mitochondria by site-specific photocrosslinking, Proc. Natl. Acad. Sci. U.S.A. 94 (1997) 485–490.

[94] J. Blom, M. Kübrich, J. Rassow, W. Voos, P.J. Dekker, A.C. Maarse, M. Meijer, N. Pfanner, The essential yeast protein MIM44 (encoded by MPI1) is involved in an early step of preprotein translocation across the mitochondrial inner membrane, Mol. Cell. Biol. 13 (1993) 7364–7371.

[95] H.C. Schneider, J. Berthold, M.F. Bauer, K. Dietmeier, B. Guiard, M. Brunner, W. Neupert, Mitochondrial Hsp70/MIM44 complex facilitates protein import, Nature 371 (1994) 768–774.

[96] N.G. Kronidou, W. Oppliger, L. Bolliger, K. Hannavy, B.S. Glick, G. Schatz, M. Horst, Dynamic interaction between Isp45 and mitochondrial hsp70 in the protein import system of the yeast mitochondrial inner membrane, Proc. Natl. Acad. Sci. U.S.A. 91 (1994) 12818–12822.

[97] H.C. Schneider, B. Westermann, W. Neupert, M. Brunner, The nucleotide exchange factor MGE exerts a key function in the ATP-dependent cycle of mt-Hsp70–Tim44 interaction driving mitochondrial protein import, EMBO J. 15 (1996) 5796–5803.

[98] R. Josyula, Z. Jin, Z. Fu, B. Sha, Crystal structure of yeast mitochondrial peripheral membrane protein Tim44p C-terminal domain, J. Mol. Biol. 359 (2006) 798–804.

[99] N. Handa, S. Kishishita, S. Morita, R. Akasaka, Z. Jin, J. Chrzas, L. Chen, Z.J. Liu, B.C. Wang, S. Sugano, A. Tanaka, T. Terada, M. Shirouzu, S. Yokoyama, Structure of the human Tim44 C-terminal domain in complex with pentaethylene glycol: ligand-bound form, Acta Crystallogr. D63 (2007) 1225–1234.

[100] M. Marom, R. Safonov, S. Amram, Y. Avneon, E. Nachliel, M. Gutman, K. Zohary, A. Azem, Y. Tsfadia, Interaction of the Tim44 C-terminal domain with negatively charged phospholipids, Biochemistry 48 (2009) 11185–11195.

[101] M. Blamowska, M. Sichting, K. Mapa, D. Mokranjac, W. Neupert, K. Hell, ATPase domain and interdomainlinker play a key role in aggregation of mitochondrial Hsp70 chaperone Ssc1, J. Biol. Chem. 285 (2010) 4423–4431.

[102] O. Gakh, P. Cavadini, G. Isaya, Mitochondrial processing peptidases, Biochim. Biophys. Acta 1592 (2002) 63–77.

[103] F.-N. Vögtle, S. Wortelkamp, R.P. Zahedi, D. Becker, C. Leidhold, K. Gevaert, J. Kellermann, W. Voos, A. Sickmann, N. Pfanner, C. Meisinger, Global analysis of the mitochondrial N-proteome identifies a processing peptidase critical for protein stability, Cell 139 (2009) 428–439.

[104] A.B. Taylor, B.S. Smith, S. Kitada, K. Kojima, H. Miyaura, Z. Otwinowski, A. Ito, J. Deisenhofer, Crystal structures of mitochondrial processing peptidase reveal the mode for specific cleavage of import signal sequences, Structure 9 (2001) 615–625.

[105] B.W. Matthews, Structural basis of the action of thermolysin and related zinc peptidases, Acc. Chem. Res. 21 (1988) 333–340.

[106] C.M. Koehler, S. Merchant, G. Schatz, How membrane proteins travel across the mitochondrial intermembrane space, Trends Biochem. Sci. 24 (1999) 428–432.

[107] M.F. Bauer, S. Hofmann, W. Neupert, M. Brunner, Protein translocation into mitochondria: the role of TIM complexes, Trends Cell Biol. 10 (2000) 25–31.

[108] S.C. Hoppins, F.E. Nargang, The Tim8–Tim13 complex of *Neurospora crassa* functions in the assembly of proteins into both mitochondrial membranes, J. Biol. Chem. 279 (2004) 12396–12405.

[109] N. Wiedemann, K.N. Truscott, S. Pfannschmidt, B. Guiard, C. Meisinger, N. Pfanner, Biogenesis of the protein import channel Tom40 of the mitochondrial outer membrane: intermembrane space components are involved in an early stage of the assembly pathway, J. Biol. Chem. 279 (2004) 18188–18194.

[110] N. Wiedemann, N. Pfanner, M.T. Ryan, The three modules of ADP/ATP carrier cooperate in receptor recruitment and translocation into mitochondria, EMBO J. 20 (2001) 951–960.

[111] C.T. Webb, M.A. Gorman, M. Lazarou, M.T. Ryan, J.M. Gulbis, Crystal structure of the mitochondrial chaperone Tim9•10 reveals a six-bladed a-propeller, Mol. Cell 21 (2006) 123–133.

[112] M.J. Baker, C.T. Webb, D.A. Stroud, C.S. Palmer, A.E. Frazier, B. Guiard, A. Chacinska, J.M. Gulbis, M.T. Ryan, Structural and functional requirements for activity of the Tim9–Tim10 complex in mitochondrial protein import, Mol. Biol. Cell 20 (2009) 769–779.

[113] K.N. Beverly, M.R. Sawaya, E. Schmid, C.M. Koehler, The Tim8–Tim13 complex has multiple substrate binding sites and binds cooperatively to Tim23, J. Mol. Biol. 382 (2008) 1144–1156.

[114] R. Siegert, M.R. Leroux, C. Scheufler, F.U. Hartl, I. Moarefi, Structure of the molecular chaperone prefoldin: unique interaction of multiple coiled coil tentacles with unfolded proteins, Cell 103 (2000) 621–632.

[115] T.A. Walton, M.C. Sousa, Crystal structure of Skp, a prefoldin-like chaperone that protects soluble and membrane proteins from aggregation, Mol. Cell 15 (2004) 367–374.

[116] I.P. Korndorfer, M.K. Dommel, A. Skerra, Structure of the periplasmic chaperone Skp suggests functional similarity with cytosolic chaperones despite differing architecture, Nat. Struct. Mol. Biol. 11 (2004) 1015–1020.

[117] V.F. Lundin, P.C. Stirling, J. Gomez-Reino, J.C. Mwenifumbo, J.M. Obst, J.M. Valpuesta, M.R. Leroux, Molecular clamp mechanism of substrate binding by hydrophobic coiled-coil residues of the archaeal chaperone prefoldin, Proc. Natl. Acad. Sci. U.S.A. 101 (2004) 4367–4372.

[118] M. Naoé, Y. Ohwa, D. Ishikawa, C. Ohshima, S. Ishikawa, H. Yamamoto, T. Endo, Identification of Tim40 that mediates protein sorting to the mitochondrial intermembrane space, J. Biol. Chem. 279 (2004) 47815–47821.

[119] A. Chacinska, S. Pfannschmidt, N. Wiedemann, V. Kozjak, L.K. Sanjuán-Szklarz, A. Schulze-Specking, K.N. Truscott, B. Guiard, C. Meisinger, N. Pfanner, Essential role of Mia40 in import and assembly of mitochondrial intermembrane space proteins, EMBO J. 23 (2004) 3735–3746.

[120] N. Mesecke, N. Terziyska, C. Kozany, F. Baumann, W. Neupert, K. Hell, J.M. Herrmann, A disulfide relay system in the intermembrane space of mitochondria that mediates protein import, Cell 121 (2005) 1059–1069.

[121] M. Rissler, N. Wiedemann, S. Pfannschmidt, K. Gabriel, B. Guiard, N. Pfanner, A. Chacinska, The essential mitochondrial protein Erv1 cooperates with Mia40 in biogenesis of intermembrane space proteins, J. Mol. Biol. 353 (2005) 485–492.

[122] D. Milenkovic, T. Ramming, J.M. Müller, L.-S. Wenz, N. Gebert, A. Schulze-Specking, D. Stojanovski, S. Rospert, A. Chacinska, Identification of the Signal directing Tim9 and Tim10 into the intermembrane space of mitochondria, Mol. Biol. Cell 20 (2009) 2530–2539.

[123] D.P. Sideris, N. Petrakis, N. Katrakili, D. Mikropoulou, A. Gallo, S. Ciofi-Baffoni, L. Banci, I. Bertini, K. Tokatlidis, A novel intermembrane space targeting signal docks cysteines onto Mia40 during mitochondrial oxidative folding, J. Cell Biol. 187 (2009) 1007–1022.

[124] S.R. Farrell, C. Thorpe, Augmenter of liver regeneration: a flavin-dependent sulfhydryl oxidase with cytochrome c reductase activity, Biochemistry 44 (2005) 1532–1541.

[125] S. Allen, V. Balabanidou, D.P. Sideris, T. Lisowsky, K. Tokatlidis, Erv1 mediates the Mia40-dependent protein import pathway and provides a functional link to the respiratory chain by shuttling electrons to cytochrome c, J. Mol. Biol. 353 (2005) 937–944.

[126] D.V. Dabir, E.P. Leverich, S.K. Kim, F.D. Tsai, M. Hirasawa, D.B. Knaff, C.M. Koehler, A role for cytochrome c and cytochrome c peroxidase in electron shuttling from Erv1, EMBO J. 26 (2007) 4801–4811.

[127] K. Bihlmaier, N. Mesecke, N. Terzyska, M. Bien, K. Hell, J.M. Herrmann, The mitochondrial disulfide relay system is connected to the electron transport chain, J. Cell Biol. 179 (2007) 389–395.

[128] N. Terziyska, T. Lutz, C. Kozany, D. Mokranjac, N. Mesecke, W. Neupert, J.M. Herrmann, K. Hell, Mia40, a novel factor for protein import into the intermembrane space of mitochondria is able to bind metal ions, FEBS Lett. 579 (2005) 179–184.

[129] S. Hofmann, U. Rothbauer, N. Mühlenbein, K. Baiker, K. Hell, M.F. Bauer, Functional and mutational characterization of human MIA40 acting during import into the mitochondrial intermembrane space, J. Mol. Biol. 353 (2005) 517–528.

[130] A. Chacinska, B. Guiard, J.M. Müller, A. Schulze-Specking, K. Gabriel, S. Kutik, N. Pfanner, Mitochondrial biogenesis, switching the sorting pathway of the intermembrane space receptor Mia40, J. Biol. Chem. 283 (2008) 29723–29729.

[131] L. Banci, I. Bertini, C. Cefaro, S. Ciofi-Baffoni, A. Gallo, M. Martinelli, D.P. Sideris, N. Katrakili, K. Tokatlidis, MIA40 is an oxidoreductase that catalyzes oxidative protein folding in mitochondria, Nat. Struct. Mol. Biol. 16 (2009) 198–206.

[132] S. Kawano, K. Yamano, M. Naoé, T. Momose, K. Terao, S. Nishikawa, N. Watanabe, T. Endo, Structural basis of yeast Tim40/Mia40 as an oxidative translocator in the mitochondrial intermembrane space, Proc. Natl. Acad. Sci. U.S.A. 106 (2009) 14403–14407.

[133] E. Vitu, M. Bentzur, T. Lisowsky, C.A. Kaiser, D. Fass, Gain of function in an ERV/ALR sulfhydryl oxidase by molecular engineering of the shuttle disulfide, J. Mol. Biol. 362 (2006) 89–101.

[134] C.K. Wu, T.A. Dailey, H.A. Dailey, B.C. Wang, I.P. Rose, The crystal structure of augmenter of liver regeneration: a mammalian FAD-dependent sulfhydryl oxidase, Protein Sci. 12 (2003) 1109–1118.

[135] D. Fass, The Erv family of sulfhydryl oxidases, Biochim. Biophys. Acta 1783 (2008) 557–566.

[136] A. Levitan, A. Danon, T. Lisowsky, Unique features of plant mitochondrial sulfhydryl oxidase, J. Biol. Chem. 279 (2004) 20002–20008.

[137] P. Kovermann, K.N. Truscott, B. Guiard, P. Rehling, N.B. Sepuri, H. Müller, R.E. Jensen, R. Wagner, N. Pfanner, Tim22, the essential core of the mitochondrial protein insertion complex, forms a voltage-activated and signal-gated channel, Mol. Cell 9 (2002) 363–373.

[138] S. Kutik, D. Stojanovski, L. Becker, T. Becker, M. Meinecke, V. Krüger, C. Prinz, C. Meisinger, B. Guiard, R. Wagner, N. Pfanner, N. Wiedemann, Dissecting membrane insertion of mitochondrial β-barrel proteins, Cell 132 (2008) 1011–1024.

[139] B. van der Berg, W.M. Clemons Jr, I. Collinson, Y. Modis, E. Hartmann, S.C. Harrison, T.A. Rapoport, X-ray structure of a protein-conducting channel, Nature 427 (2003) 36–44.

[140] J. Zimmer, Y. Nam, T.A. Rapoport, Structure of a complex of the ATPase SecA and the protein-translocation channel, Nature 455 (2008) 936–943.

[141] T. Tsukazaki, H. Mori, S. Fukai, R. Ishitani, T. Mori, N. Dohmae, A. Perederina, Y. Sugita, D.G. Vassylyev, K. Ito, O. Nureki, Conformational transition of Sec machinery inferred from bacterial SecYE structures, Nature 455 (2008) 988–991.